



**Universidade de Aveiro** Departamento de Engenharia Mecânica  
2014

**Marta García Padilla**

**Optimization of thin sheet structures with patterns perforations**





**Marta García Padilla**

**Optimization of thin sheet structures with patterns perforations**

Dissertação apresentada à Universidade de Aveiro para cumprimento dos requisitos necessários à obtenção do grau de Mestre em Engenharia Mecânica, realizada sob a orientação científica do Doutor António Gil D'Orey de Andrade Campos, Professor Auxiliar do Departamento de Engenharia Mecânica da Universidade de Aveiro.



## **o júri**

presidente

Professor Doutor Francisco José Malheiro Queirós de Melo  
Professor Associado, Universidade de Aveiro

Professor Doutor Robertt Angelo Fontes Valente  
Professor Auxiliar, Universidade de Aveiro

Professor Doutor António Gil D'Orey de Andrade Campos  
Professor Auxiliar, Universidade de Aveiro



## **agradecimientos**

A mi tutor el professor Doutor António Gil D'Orey Andrade Campos, por su apoyo, comprensión, paciencia y enseñanzas.

A mi compañero de la Universidad de Aveiro Nelson Souto, por ofrecerme su ayuda siempre que la he necesitado.

A todos mis amigos, por haberme apoyado durante todos estos años sin dejar que me desanimara y creyendo en mí. En especial a Lucas, Laura E., Laura G. y Blanca.

Y principalmente, agradecer a mi familia, por todo su apoyo y la confianza depositada en mí durante toda mi carrera. En especial a mis padres, Rafael y Marisa, por brindarme esta oportunidad y sobre todo, por la gran educación recibida que me ha permitido llegar hasta aquí.





**Key-words**

Metal storage systems, Optimization, stiffness, numerical simulation, steel.

**abstract**

Nowadays, metal storage systems are generally used in industrial companies. The several stages of the metallic structures design are based in the standard EN 15512:2009. However, this standard do not the most efficient design solution, only design constraints.

In this work, it is intended to improve the structural elements that are on the base of the metal storage systems, particularly shelves, in order to reduce costs and increase the structure stiffness, enforcing the international standard that define the characteristics of these products. The main purpose is the optimization of a representative section of profiled steel component taking into account the variable thickness, geometry and number of perforations.

In order to do this a computational finite element model is developed and pre-validated, replacing a numerous set of experimental tests in a design of Experiments (DoE) methodology. The optimized solutions were obtained through a response surface optimization methodology (RSM). The final results were analysed and discussed.



**palavras-chave**

Sistemas metálicos de armazenamento, Otimização, rigidez, simulação numérica, aço.

**resumo**

Hoje em dia, os sistemas metálicos de armazenamento são vulgarmente utilizados pela indústria. As várias etapas de projeto destas estruturas metálicas são baseadas na norma EN 15512:2009. No entanto, esta norma não propõe a solução de projeto mais eficiente, apenas as suas restrições.

Neste trabalho, pretende-se aperfeiçoar os elementos estruturais que estão na base dos sistemas de armazenamento de metal, particularmente prateleiras, a fim de reduzir custos e aumentar a rigidez da estrutura, satisfazendo a norma internacional que define as características necessárias desses produtos. O objetivo principal é a otimização de uma secção representativa do componente de aço perfilado tendo em conta as variáveis espessura, geometria e número de perfurações.

Para isso, é desenvolvido e validado um modelo computacional de elementos finitos, substituindo um numeroso conjunto de testes experimentais numa metodologia de *Design of Experiments* (DoE). As soluções otimizadas são obtidas através de uma metodologia de otimização baseada numa superfície de resposta (RSM). Os resultados finais são analisados e discutidos





## Contents

I. Guidelines .....	15
1. Introduction.....	17
1.1. Context.....	17
1.2. Objectives.....	17
2. State-of-the-art.....	18
2.1. Standards for the design of metal shelves structures: calculation procedures ...	18
2.2. Documentation review .....	30
II. Methods and development .....	39
3. Methodology .....	41
3.1. Optimisation problem formulation .....	41
3.1.1. Design of experiments (DOE) .....	41
3.1.2. Response surface method (RSM) .....	42
III. Results .....	45
4. Description of the problem .....	47
5. Modelling.....	49
6. Experimental results.....	51
7. Model calibration .....	52
8. Optimisation formulation .....	53
9. Experiments and results .....	54
10. RSM and final value .....	60
IV. Conclusion .....	69
11. Conclusions.....	71
Bibliography .....	73







## PART

### **I. Guidelines**



## **1. Introduction**

### **1.1. Context**

The structures are the basic element of all construction and its function is to receive and transmit weight and external forces to the ground, so that all elements are in balance. The transmission of such efforts is achieved by internal stress and its distribution along the structural parts.

Engineering structures are so varied that any attempt to list them is a challenge, except in a very general way. The innumerable problems that arise in their design have caused engineers to specialize in individual designs or in groups of similar structures. Therefore the study here is contested in the area of expertise of metal storage structures

### **1.2. Objectives**

Nowadays, metal storage systems are general structures often used in industry. The several stages of the metallic structures design are based in the standard EN 15512:2009, that details the failure modes of the major elements, including beams (see section 2.1.). However, this standard do not the most efficient design solution, only design constraints. In this work, it is intended to improve the structural elements that are on the base of the metal storage systems, particularly shelves, in order to reduce costs and increase the structure stiffness, enforcing the international standard that define the characteristics of these products.

The main purpose is the optimization of a representative section of profiled steel component taking into account the variable thickness, geometry and number of perforations.

In order to do this a computational finite element model is developed and pre-validated, replacing a numerous set of experimental tests in a design of Experiments (DoE) or Taguchi's methodology. The numerical model is also used to study the buckling behaviour of the columns and their bending behavior. Using a response surface optimization methodology (RSM), the optimized solutions are obtained.

## **2. State-of-the-art**

In this section, a brief review is made concerning the standard and works by other authors. Some comments related to the influence of the standard in the structures of this work are made.

### **2.1. Standards for the design of metal shelves structures: calculation procedures**

In order to design the steel structure the engineer must have knowledge about the calculation procedure on metal shelves based on the standard EN 15512:2009.

The following steps summarize the procedure to design:

#### **1. *Definition of the characteristics of the structures***

Initially it must be defined the main characteristics of the structure:

- Profiles;
- Length of the beams and columns;
- Bracing;

These profiles should satisfy the point 8 of the standard EN 15512:2009, that is related to the selected material. For this work the use of standard steel satisfy this point.

#### **2. *Calculation of Structural Properties of profiles***

Section 9 of the standard EN 15512:2009 requires to be taken into account some structural properties of the radius of curvature in sections and holes along the profiles.

#### **3. *Definition of the actions to consider in the design procedure***

In section 6 of the standard EN 15512:2009 there is a classification of actions: permanents (resulting from the weight of the profiles) and variables (weights of the materials stored, accidental impact loads and others).

In fact, the vertical alignment imperfections can be modelled by horizontal loads applied to the structure (sections 5.3.2, 5.3.3 and 5.3.5).

The global analysis of the structure is based on various combinations of actions defined to evaluate:

- Yield state
- Service limit state
- Global stability under a single horizontal load

#### **4. *Global analysis of the structure***

At first it is necessary to use second-order theories, mandatory for unconstrained structures (un-braced) in the longitudinal direction (down-aisle). Structures with encastre (braced) can be analysed with first order paragraph 10.3.3 conditions are checked.

The 3D analysis with calculation programs is more rigorous, however section 10 allows the standard 2D analysis in longitudinal planes (down-aisle) and transverse (cross-aisle), still requiring to consider interactions between plans.

#### **5. *Verification of the members***

By the global analysis of the structure the efforts which govern each member are obtained, and then the various failure modes must be checked.

The standard EN 15512:2009 details the following failure modes of the major elements, for the beams (section 9.4):

- Plastic failure
- Maximum displacement (EN 1993:1-3)
- Web crippling
- Lateral buckling under bending-torsion (section 9.6)

And for the columns:

- Bending (chapters 9.7.3., 9.7.6.2., 9.7.6.3., 9.7.6.5.)
- Flexural buckling (chapters 9.7.4., 9.7.5., 9.7.6.4., 9.2.4., 9.2.5.)

Finally, it is necessary to check for other elements:

- The beam-columns connections (section 9.5);
- Connection elements between beam and column (splices) (section 9.8)
- The ground plates connections (section 9.9)
- Connection elements between pillars (section 9.11)

Considering that for this work section 8 and 9 are critical, a small description of these sections are useful.

### **2.1.1. Dimensional tolerances**

#### **1. *Thickness of materials***

The design rules given in the chapter 8.5.2. of this standard shall be limited to the following core thickness  $t_c$  exclusive of coatings unless specified otherwise, where:

$$0.5 \leq t_c \leq 8.0 \text{ mm.} \quad (2.1.)$$

### **2.1.2. Calculation of section properties**

#### **1. Effect of cross-section distortion as defined in section 9.2.4 of the standard**

Compression members of the open cross-section are subject to three buckling modes, which are, in order of wavelength (see EN 1993-1-3):

- a) Local buckling
- b) Distortional buckling
- c) Lateral torsional buckling

For members of intermediate effective length, as are generally encountered in the upright frames of typical pallet racks, the distortional mode is likely to be the most critical. If the member is perforated, its performance with respect to distortional buckling shall be determined by test. If the member is not perforated, two cases shall be considered, shown at this point in the standard EN15512:2009.

It should be noted that distortional buckling is extremely sensitive to the end conditions (fixed or simply supported with respect to the distortional mode) and care should be taken to ensure that the boundary conditions in either analysis or testing correspond to those in the prototype member. The wavelength for distortional buckling is significantly longer than that for local buckling. This means that distortional buckling is not usually identified by a conventional stub-column test. Furthermore, if a stub-column test exhibits a distortional failure mode, it is unlikely that the length is sufficient to determine the minimum distortional buckling load (for more details, sections Annex A.2.2 for the standard).

#### **2. Effect of local buckling (shown in section 9.2.5. of the standard)**

Thin walled elements in compression are prone to local buckling. When calculating the load bearing capacity and stiffness, the effect of local buckling shall be taken into account by using the effective cross-sectional properties calculated on the basis of the effective width of individual elements in compression. Effective section properties are used in strength calculations and shall be calculated for non-perforated members in accordance with EN 1993-1-3 or determined by stub column tests according to A.2.1.

Compression elements with perforations shall be designed on the basis of tests (see A.2.1, A.2.2, A.2.3).

Compression elements without perforations may be assumed to be fully effective if the width to thickness ratio complies the limits shown in the standard.

### 2.1.3. Design of beams (described in section 9.4 of the standard)

#### 1. General:

The beam length considered to beam check analysis, may be taken as the distance between the faces of the two adjacent uprights.

Beams shall be considered at the ultimate limit and serviceability limit states as follows.

- a) Ultimate limit state.
- b) Serviceability limit state.

2. **Loads on beams:** Distributed load is considered if not otherwise specified.

#### 3. Design bending moments for beams

##### 3.1. General:

If the restraining effect of the beam end connector is taken into account, then the design moments may be taken directly from the results of a second-order analysis at the design load factor. In frames with sway, the design bending moments at the centre of the beam may be obtained from a first-order analysis.

Plastic design of the beams may be used, even if global stability is justified on the basis of elastic design, provided that proper consideration is given to the rotation capacity of the beam end connector.

##### 3.2. Redistribution of bending moments in the case of elastic analysis:

If an elastic analysis with linear connector behaviour shows that the ultimate moment of resistance of one or both beam end connections is exceeded, the bending moment may be redistributed in the beam and the associated beam end by up to 15% of the end moment, as shown in the Figure 2.1.

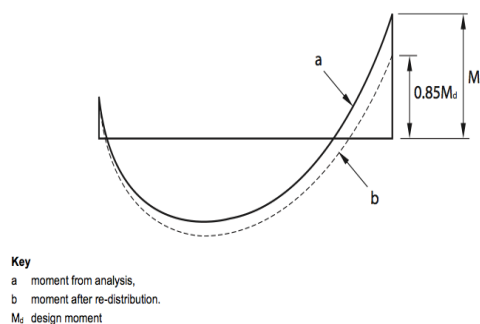


Figure 2.1. – Representation of the redistribution of the bending moment.

### 3.3. Approximate design:

An alternative design for a symmetrically loaded beam section shall be to consider the most heavily loaded beam of its type.

### 4. Design shear force for beams:

In racks which are braced against sway, the design shear force for the beam and beam end connector shall be obtained from either a first-order or second-order global analysis. In racks which are free to sway, the design shear force shall be obtained from a second-order analysis.

### 5. Deflection of beams:

In the serviceability limit state the maximum deflection of any beam shall be obtained from either a first- or second-order analysis which takes due account of pattern loading.

For racks of regular construction and loading, the maximum deflection may be taken as:

$$\Delta_{\max} = \frac{5W_{\text{ser}}L^3}{384EI_b} \beta_{\Delta} \left( 1 - \frac{0.8\beta_{\theta}}{\beta_{\Delta} \left[ 1 + \frac{2EI_b}{k_e L} \right]} \right) \quad \begin{array}{l} W_{\text{ser}} = \text{the total serviceability load per beam;} \\ \beta_{\theta} \text{ and } \beta_{\Delta} \text{ are according to Annex G.} \end{array} \quad (2.2.)$$

### 6. Beams as tie beams in braced pallet racks:

For pallet racking systems incorporating spine bracing the beams have an additional function of tying the upright with the bracing system and as a result carry an additional compressive or tensile load.

### 7. Design resistance with respect to web crippling:

Design of beams with respect to web crippling arising from a local load or support reaction shall be carried out in accordance with the guidance given in EN 1993-1-3.

### 8. Design resistance with respect to shear forces:

Design of beams with respect to shear forces shall be carried out in accordance with the guidance given in EN 1993-1-3.

### 9. Combined shear force, axial force and bending moment:

Design of beams with respect to combined shear forces, axial force and bending moment shall be carried out in accordance with the guidance given in EN 1993-1-3.



### 10. Combined bending moment and web crippling:

Design of beams with respect to combined bending moment and web crippling arising from a local load or support reaction shall be carried out in accordance with the guidance given in EN 1993-1-3.

#### 2.1.4. Beams subject to bending and torsion, as is described in section 9.6 of the standard

##### 1. General:

When warping stresses arise as a result of torsional effects, the design shall either be carried out on the basis of tests or, alternatively, by calculation according to EN 1993-1-3.

##### 2. Lateral torsional buckling of beams:

The design strength  $M_{b,Rd}$  of beams subject to lateral torsional buckling shall be determined either by tests according to A.2.10 or by calculation shown at this point with equations 22,23 and 24 of the standard.

The use of buckling curve 'b' is considered to be generally applicable to pallet rack beams. However this factor may vary depending on the shape of the profile. Further guidance is given in EN 1993-1-3.

The calculation of  $M_{cr}$  shall be based on the gross cross-section (for sections which are symmetrical about the minor axis, see EN 1993-1-1) using an effective length equal to the beam length.

#### 2.1.5. Compression, tension and bending in members (section 9.7 of the standard)

##### 1. Cross-sectional verification:

Under uniform compression, the following condition shall be verified:

$$N_{Sd} \leq N_{c,Rd} \quad (2.3.)$$

Where:

$$\left\{ \begin{array}{l} N_{Sd} = \text{compressive force due to design load} \\ N_{c,Rd} = \frac{f_y A_{eff}}{\gamma_M} \\ A_{eff} = \text{effective cross-sectional area for uniform compression} \\ \gamma_M \text{ in accordance with 7.5} \end{array} \right. \quad (2.4.)$$

Any shift of the centroid of the effective area relative to the centre of gravity of the gross cross section in the design of the uprights of typical pallet racking structures need not be taken into account.

## **2. Design strength with respect to flexural buckling**

### 2.1. General

The design buckling resistance  $N_{b,Rd}$  shall be determined as is shown in equations 26, 27, 28 and 29 of the standard at this point.

### 2.2. Buckling curves

Four buckling curves, (*i.e.* relationships between design stress and slenderness) are available, depending on the type of cross-section and the plane of buckling. The buckling curves are each associated with a value of the imperfection factor  $\alpha$  given in Table 8 and the appropriate buckling curve for a particular section shall be determined from Table 9.

If Built-up closed sections shall be checked using either:

a) The basic yield strength  $f_{yb}$  of the flat sheet material out of which the member is made by cold-forming, with buckling curve b.

b) The average yield strength  $f_{ya}$  of the member after cold-forming, determined in conformity with the definition given in 8.2 with buckling curve c.

If the buckling curve is determined by tests according to A.2.3 then that buckling curve may be used.

### 2.3. Buckling length

The buckling length  $l$  for a given member which is an element of a system shall be determined as the length of a column of the same cross-section and with both ends pinned which has the same Euler critical load as the system under consideration.

If the axial forces and bending moment in the plane of buckling of a member have been determined on the basis of a second-order analysis, they are already enhanced by second-order effects and the buckling length may be considered as equal to the system length. When second-order global analysis is used, it is permissible to use in-plane buckling lengths for the non-sway mode for member design.

The determination of the buckling length which follows is applicable to the members of braced frames and frames for which no second-order analysis is available.

The buckling length  $l$  of a member in compression may be determined by either rational analysis or testing giving due regard to the behaviour of the complete frame and the nature of the restraints provided at connections of bracing members or other restraining elements.

If the buckling length has not been determined by global analysis, the following values of the effective length factor K shall be used, where:

$$\ell = KL \quad (2.5.)$$

L = system length

Then the factor K will be:

a) For any member with both ends held in position with regard to the buckling mode under consideration:  $K = 1$ .

b) For the bottom length of an upright in a braced upright frame in the cross-aisle direction.

Provided that: bracing members are connected to both flanges of the upright, bracing eccentricities satisfy the requirements of 8.6 and 8.7, a base plate is fitted to the upright and the floor is concrete. The value of K will be:  $K=0,9$

If the above conditions except the third or fourth are satisfied,  $K=10$ .

NOTE In a braced frame, if the bottom node is not near the floor (see 8.6), the length between the floor and the first node should be considered as being free to sway.

c) For all other parts of the upright in a braced upright frame in the cross-aisle direction:  $K=1$

d) For horizontal and diagonal bracing members in an upright frame. Provided the bracing member is welded with a fillet weld of length at least 20 mm to both flanges of the uprights:  $K=0,9$  (only for in plane buckling).

For all other cases:  $K=1$

If the connections at the ends of a bracing member do not coincide with its system lines, the member shall be designed for combined axial load and bending.

e) For frames braced in the down-aisle direction (spine braced frames), the factor K is the same as that for the cross-aisle direction given in b) and c).

For the bottom column length, there are three cases to consider.

f) For frames un-braced in the down-aisle direction. When a second-order analysis is carried out overall stability is taken into account in the enhanced bending moments and it is therefore conservative to design using  $K = 1$  with values of L given in e) above.

### **3. Torsional and flexural-torsional buckling**

#### **3.1: General**

Torsional buckling is usually only critical for point-symmetric open sections. Mono-symmetric and non-symmetric sections are generally subject to flexural-torsional buckling.

In addition to checking for flexural-torsional buckling, flexural buckling about the weaker principal axis should also be checked.

3.2: Design strength with respect to torsional and flexural-torsional buckling

The design buckling resistance  $N_{b,Rd}$  corresponding to torsional or flexural-torsional buckling shall be determined by using the expressions given in 9.7.4 by substituting the lesser of  $N_{cr,T}$  or  $N_{cr,FT}$  for  $N_{cr}$ , with:

$$N_{cr,T} = \frac{1}{i_o^2} \left( G I_T + \frac{\pi^2 E I_w}{L_{eT}^2} \right) \text{ critical force for torsional buckling} \quad (2.6.)$$

$$N_{cr,FT} = \frac{N_{cr,y}}{2\beta} \left[ 1 + \frac{N_{cr,T}}{N_{cr,y}} - \sqrt{\left( 1 - \frac{N_{cr,T}}{N_{cr,y}} \right)^2 + 4 \left( \frac{y_o}{i_o} \right)^2 \frac{N_{cr,T}}{N_{cr,y}}} \right] \quad (2.7.)$$

NOTE: The second expression applies only for cross-sections that are symmetrical about the y-y axis (e.g.  $z_0 = 0$ ). For other sections, guidance should be obtained from literature.

With:

$$\beta = 1 - \left( \frac{y_o}{i_o} \right)^2 \quad (2.8.)$$

Where:  $\left\{ \begin{array}{l} N_{cr,FT} = \text{critical force for flexural - torsional buckling} \\ N_{cr,y} \text{ is the elastic critical load of the upright based on buckling lengths according to 9.7.4.3.} \end{array} \right.$

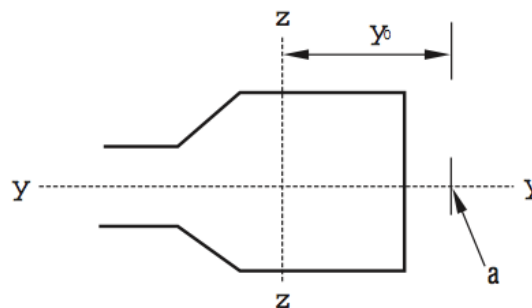


Figure 2.2. – Schema of cross-section

$$\left\{ \begin{array}{l}
 a = \text{shear centre} \\
 Ag = \text{area of the gross cross – section} \\
 i_0^2 = i_y^2 + i_z^2 + y_0^2 \\
 E = \text{modulus of elasticity} \\
 G = \text{shear modulus} \\
 B = 1 - \left(\frac{y_0}{i_0}\right)^2 \\
 y_0 = \text{distance along the } y - \text{axis from} \\
 \quad \text{the shear centre to the centre of} \\
 \quad \text{gravity of the gross cross – section} \\
 i_y, i_z = \text{radii of gyration of the gross cross –} \\
 \quad \text{section about the } y \text{ and } z \text{ axes respectively} \\
 IT = \text{St Venant torsional constant of the gross cross – section} \\
 I_w = \text{warping constant of the gross cross – section} \\
 LeT = \text{effective length of the member with respect to twisting}
 \end{array} \right.$$

#### 4. Combined bending and axial loading

##### 4.1. Bending and axial compression

For members in combined compression and bending, shall be satisfied the condition in section 9.7.6.2..

##### 4.2. Bending and axial compression without lateral-torsional buckling

In addition to satisfying 9.7.6.2 members subject to combined bending and axial compression shall also satisfy.

$$\frac{N_{sd}}{X_{min} A_{eff} / \gamma_M} + \frac{k_y M_{y, sd}}{W_{eff, y} f_y / \gamma_M} + \frac{k_z M_{z, sd}}{W_{eff, z} f_y / \gamma_M} \leq 1 \quad (2.9.)$$

Where:

$$k_y = 1 - \frac{\mu_y N_{sd}}{X_y A_{eff} f_y} \quad \text{but} \quad k_y \leq 1,5 \quad (2.10.)$$

$$\mu_y = \bar{\lambda}_y (2\beta_{M, Z} - 4) \quad \text{but} \quad \mu_y \leq 0,9 \quad (2.11.)$$

$$k_z = 1 - \frac{\mu_z N_{sd}}{X_z A_{eff} f_z} \quad \text{but} \quad k_z \leq 1,5 \quad (2.12.)$$

$$\mu_z = \bar{\lambda}_z (2\beta_{M, Z} - 4) \quad \text{but} \quad \mu_z \leq 0,9 \quad (2.13.)$$

- $\chi_{min}$  = the lesser of  $\chi_{db}$ ,  $\chi_y$  and  $\chi_z$ ; where  $\chi_{db}$  is the reduction factor calculated in 9.7.2.c and  $\chi_y$  and  $\chi_z$  are the reduction factors from 9.7.4 for the y- y and z- z axes respectively. The influence of any distortional buckling effects should be taken into account.
- $N_{db,Rd} = N_{crit} = \chi_{min} A_{eff} f_y$  may be determined as the characteristic value of resistance obtained from compression test on upright sections according to A.2.3 or by calculation based on stub column tests provided that distortional buckling effects are taken into account in accordance with 9.7.2.
- $\beta_{M,y}$  and  $\beta_{M,z}$  are equivalent uniform moment factors for flexural buckling, (see 9.7.6.4). If the stress resultants arise as a result of a second-order analysis with global imperfections,  $k_y$  and/or  $k_z$  is not greater than 1. But if the stress resultants arise with global and local imperfections,  $\chi_y$  and/or  $\chi_z = 1$ , as appropriate, provided that there is no effect due to distortional buckling.
- $W_{eff,y}$  is the effective section modulus of the cross-section when subject only to moment about the y-y axis.
- $W_{eff,z}$  is the effective section modulus of the cross-section when subject only to moment about the z-z axis

#### 4.3. Bending and axial compression with lateral torsional buckling

In addition to satisfying 9.7.5, members for which lateral-torsional buckling is a potential failure mode shall also satisfy:

$$\frac{N_{Sd}}{\chi_{min} A_{eff} f_y / \gamma_M} + \frac{k_{LT} M_{y,Sd}}{\chi_{LT} W_{eff,y} f_y / \gamma_M} + \frac{k_z M_{z,Sd}}{W_{eff,z} f_y / \gamma_M} \leq 1 \quad (2.14.)$$

Where:

$$k_{LT} = 1 - \frac{\mu_{LT} N_{Sd}}{\chi_z A_{eff} f_z} \quad \text{but} \quad k_{LT} \leq 1 \quad (2.15.)$$

$$\mu_{LT} = 0,15 \bar{\lambda}_z (2\beta_{M,LT} - 4) \quad \text{but} \quad \mu_{LT} \leq 0,9 \quad (2.16.)$$

- $\beta_{M,LT}$  is an equivalent uniform moment factor for lateral-torsional buckling
- $k_z$ ,  $A_{eff}$ ,  $W_{eff,y}$  and  $W_{eff,z}$  are as in 9.7.6.3
- $\chi_{min}$  is the smallest of  $\chi_{db}$  (from 9.7.2c),  $\chi_y$  and  $\chi_z$  (from 9.7.4) and of the reduction factors corresponding to the distortional and flexural-torsional buckling modes.
- $\chi_{LT}$  is the reduction factor for flexural-torsional buckling (see EN 1993-1-3).
- $\lambda_z$  is the slenderness ratio for flexural buckling.

The equivalent uniform moment factors  $\beta_{M,Y}$ ,  $\beta_{M,Z}$  and  $\beta_{M,LT}$  shall be obtained from Figure 25 according to the shape of the bending moment diagram between braced points as in Table 10, which are at this point at the standard EN15512:2009.

## 4.2. Bending and axial tension

### 4.2.1. Tension only

Hot rolled tension members shall be designed in accordance with Clause 6.2.3 of EN 1993-1-1. Cold-formed tension members shall be designed in accordance with Clause 6.1.2 of EN 1993-1-3.

### 4.2.2. Combined bending and tension

For members in combined bending and tension, the following condition shall be satisfied:

$$\frac{N_{Sd}}{N_{t,Rd}} + \frac{M_{y,Sd}}{M_{cy,Rd}} + \frac{M_{z,Sd}}{M_{cz,Rd}} \leq 1 \quad (2.16)$$

Where  $M_{sd}$  and  $N_{sd}$  are design values of moment and tensile force respectively and the resistance terms are defined in 9.3.2. and 9.7.6.5.1

### 2.1.6. Design of splices

Splices shall be designed either by calculation or by testing according to A.2.11.

### 2.1.7. Design of base plates as defined in section 9.9 of the standard

#### 1. General

Every upright shall be fixed with a base plate. Checks shall be carried out on the strength of the base plate, the contact pressure and the holding down bolt.

Determination of the contact pressure and base plate may be carried out under the general action of the normal force. Any moments from the restraint may be ignored.

#### 2. Effective area $A_{bas}$ for base plates

The design of a concentrically loaded base plate shall assume that the bearing pressure on the effective area of the base plate is uniformly distributed over the effective area. In Figure 26 the effective area is indicated by the shaded portion and we can use the equations 40 and 42.

### **2.1.8. Design of run spacers (shown in section 9.11 of the standard)**

In double entry racks, at least two run spacers (see Figure 2) shall be provided between each adjacent pair of upright frames. These shall be located at the node points of the upright frames and spaced as widely apart as practicable.

## **2.2. Documentation review**

Recent progress in the field of cold-formed steel members with particular emphases given to progress in the field of distortional buckling can be seen in [1]. A range of use of cold-formed sections has been increased because the thickness of the plates was reduced in last years. However that generates complex design problems, particularly in the fields of structural stability and joints. In compression this kind of members can exhibit three modes of instability: local, distortional and flexural-torsional buckling. Distortional buckling is very important with thin sections made with strength steels. Nowadays, the power of computers and development of software has been increased allowing numerical simulation to be used in almost all research fields. Now computational modelling of very complex problems is already possible. The last decade has shown large and important progresses in the knowledge of the behaviour of cold-formed steel members and structures.

Two years later a review paper by G.J. Hancock [2] was done to provide an updated review of references for cold-formed steel research as published in leading journals in 1999–2001. The second objective was to describe the developments in the North American Specification (NAS) for the Design of Cold-Formed Steel Structural Members. The third objective was the introduction of the Direct Strength Method (DSM) under development for cold-formed steel structural member design.

The North American Specification for the Design of Cold-Formed Steel Structural Members has recently been published which precede the previous editions of the Specification for the Design of Cold-Formed Steel Structural Members published by the American Iron and Steel Institute, and the S136-94 Standard for Cold-Formed Steel Structural Members. It is intended for use in the USA, Canada and Mexico in a similar way that Eurocode 3 is to be used in the European Community. A major achievement of the specification is the bringing together of research throughout the world, particularly the USA, Canada and some from Australia to make the specification as up-to-date as is technically possible. The method used in the standard until 2002 to account local and distortional buckling of thin-walled in compression are based on the width method, but this method is for the study of elements in isolation, so it is not as accurate as it should.



To overcome this problem, a new method has been developed by Schafer and Peköz called the 'Direct Strength Method'. It uses elastic buckling solutions for the entire cross-section. The DSM assumes that local buckling behaviour can also be predicted using the elastic local buckling stress of the whole section with an appropriate strength design curve for local instability. The method has the advantage that calculations for complex sections are very simple [2].

In the course of time, an increasing development in this field was observed and a new method was published in July 2006. The article by Murat Pala, Naci Caglar is concerning Neural Networks [3], that is a different modelling method proposed to simplify the experimental analysis that was done in past decades to study the effect of the geometric parameters of cold-formed C-sections on distortional buckling stress, since an experimental study of cold-formed thin-wall steel members is very complex. The NN gives very good results. This method has become popular and has been used by many researchers for a variety of engineering applications. NNs are a family of massively parallel architectures that solve difficult problems via the cooperation of highly interconnected but simple computing elements. Buckling distortion of thin plate elements is very difficult to analyse analytically although in the decade of 1960 approximate analytical methods were developed. In the 1970s methods based on finite elements were introduced but formulas didn't give good enough results. In 1980s the finite strip method (FSM) appeared to calculate distortional buckling. FSM can be effectively used in structures that have regular geometry along their length and it has been efficiently used to calculate the local, distortional and flexural-torsional modes of cold-formed steel members. But there is a problem, the engineers have to work with incomplete information which is one of the areas where NNs are generally applicable. Such a trained neural network would not only be able to reproduce the experimental results it was trained on, but through its generalization capability it should be able to approximate the results of other experiments [3].

In this article [3] a neural network model is proposed to perform the analysis instead of known methods for the parametric application of distortional buckling stress.

Parametric studies are performed to verify the generalization capability of the trained NNs and to obtain the interrelationship between geometric parameters of C-section and EDBS. Good results were shown.

Another article by M.M. Pastor, M. Casafont, E. Chillarón, A. Lusa, F. Roure, M.R. Somalo [4] is focused on how the section can be optimally designed to achieve the highest possible failure load in global buckling. For this aim a set of experimental test were

presented and results of upright cross-sections in compression were discussed. It should be known that some rules for cold-formed member analysis are given, but in the case of perforated members they are not recommended, and in this research these are the kind of members for the study. However, this is not intended to restrict the development of analytical procedures (e.g. using finite elements) for predicting the performance of members containing regular arrays of holes or slots. In this article on the optimization procedure two types of shapes are studied (A and B), B-shape has more area than A-shape but the same thickness, to conclude the B-shape was better.

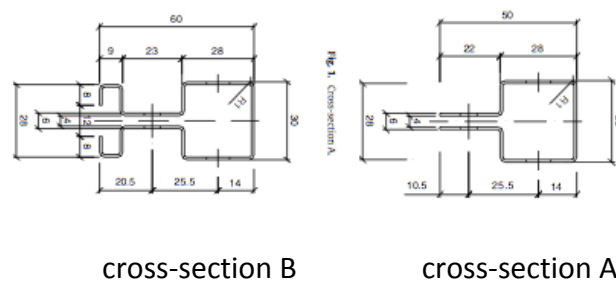


*Figure 2.3. – Cross-sections of the specimens to be tested in order to find the optimal shape.*

However, when longer specimens were tested to obtain the experimental buckling curve of the profile, it was observed that the increase in strength, reduced as the length increased. In this study both shapes with different length were analysed, first determined by applying the specifications proposed in EN 15512:2008 Standard, second by FEM nonlinear analysis (ANSYS code), and finally from experimental testing. In [4] some curves were obtained that show the standard and numerical analyses come close to the behaviour of both uprights in compression although the EN15512:2008 Standard is a little more conservative. Nonlinear buckling analysis is usually the more accurate approach, and it is therefore recommended for the design or evaluation of actual structures.

In addition a comprehensive set of experimental results from upright cross-sections subject to compression were gathered in [5]. Twenty different pallet-rack steel profiles have been tested [5]. Two alternative methods are considered: the analytical, by applying the European Standard EN 1993-1-3:2006/AC: 2009 that is a traditional method, which involves the effective width determination for each part of the section subject to compression; and the numerical, by applying finite element analysis, including non-linear material and geometrical behaviour. The results of both methods are compared to the

experimental ones. This research reveals that even though the European Standard EN 15512:2009 does only accept the experimental method for perforated sections, these other two methods can give good accuracy, and be good tools in the stage of design and optimization. During some years, the effective width method has been subject of investigation by researchers in the field of cold-formed structures because calculations would include the effects of distortional buckling. Perhaps the most important result of these investigations is the direct strength method (DSM). But these calculations can be performed by means of specific computer programs: methods based on FSM and GBT. The use of these specific programs has made the direct strength method very quick and effective. At the moment of the publication, however, they cannot be applied to perforated members. Unlike the previous article, in this paper the focus is on the buckling of short columns, that is mainly local buckling, with different shape of transversal section, thickness and shape of the holes. Concluding that although the European Standards [10,24,26] do only accept the experimental method for perforated compression members (Section 9.7.2, EN15512), this investigation confirms that the other methods, the analytical and the simulation by finite elements, come rather close to the experimental results.

Following in the field of research of steel storage racks a pilot study published in 2011 was carried out. The paper [6] addresses the problem of determining the stiffness and strength of steel storage rack base plate assemblies which are used to provide resistance against the flexural buckling. This paper provides recommendations for how best to conduct the test, and proposes an alternative test method that the one given in the EN 15512 Specification. Typically, the connection between the floor and the columns, referred to as uprights, is achieved by means of a base plate assembly, and the study is about this. The stability of a storage rack is dependent on the beam to column connection stiffness and the base plate stiffness. These both values are used in structural analysis models employed to design the storage racks order to achieve economical designs. A linear or nonlinear moment–rotation relationship is usually chosen to model the base plate connection.

Two main specifications deal with storage rack design, and they have different approaches to determining the base plate stiffness. RIM uses an equation for the base plate stiffness and the standard (EN 15512 [5]) recommends a test to determine the stiffness derived from the maximum moment observed. About these tests are two approaches: method 1 and method 2. The merits of both test set-ups are discussed, concluding that one alternative is superior to the other. In general for testing the EN 15512 Specification recommends that a range of axial loads be used in determining base plate assembly rotational stiffness and strengths. A test set-up is suggested in Section

A.2.7.2 of the Specification, and the associated Figure A.11 of the Specification is reproduced in Fig. 4 [6]. In the EN 15512 Specification, the base plate stiffness is calculated based on the characteristic failure moment ( $M_k$ ), which is derived from the maximum moments ( $M_{ti}$ ) of several tests. But when base plate tests do not reach a maximum moment, a deformation limit criterion can be used to calculate the maximum bending moment. It is proposed that a deformation limit of four times the yield deformation limit is appropriate for determining the ultimate moment from base plate tests. In this test they use the same piece with the same dimensions and varying the axial force applied. In addition an analysis of finite elements is used to compare.

On the other hand, in this same year, another study focused on determining the distortional buckling of these specimens is made. A study of these cold-formed steel columns with perforations is shown in paper by Miquel Casafont, Maria Magdalena Pastor, Francesc Roure, Teoman Peköz [7]. It is an experimental process of how the cold-forming steel columns subjected to compression is performed. Consisting of members of different lengths are measured, especially lengths members that make them subject to buckling distortion (longer than those used to measure local buckling and shorter than those used in overall buckling) but are including the member lengths used in practice. Deformation is measured and it is observed that there is a wavelength range in which the failure mode is a combination of distortion and overall buckling.

Therefore, the accuracy of the present methods would be better if a combination of both methods is made. The interaction can be taken into account in two ways: by choosing the lowest distortional buckling strength as the distortional buckling strength of the member; or by choosing the upper distortional buckling strength and applying an interaction formula; the second option is recommended.

The present investigation started with the aim of formulating a procedure to determine the length of the columns. Compression tests on different cross-sections and with different specimen lengths are carried out to find out how the appropriate test length can be selected by means of an analytical procedure, but the main goal of the paper is to show the behaviour of the members observed in the experimental tests. Different methods for the calculation of the distortional buckling strength are used: experimental results by a modification of the RMI specification approach for columns, experimental results according to the European code and by application of the direct strength method.

At the end of 2011 another study [8] concerning these specimens is carried out, but this time presents three methodologies to predict the load carrying capacity of cold-formed steel rack columns via nonlinear finite element analysis (FEA).

The analysis of these sections is currently being carried out with different methodologies. One of the most commonly used is the finite element method (FEM) but exist some problems solved through the using of the generalized beam theory (GBT). The goal of the investigation presented to determine the imperfection to be used in the FEM calculation of the ultimate load of an upright by comparing the three methods. These three numerical methodologies to predict the compression load carrying capacity of a cold-formed steel rack section (without perforations) have been analysed are:

1. First buckling mode—the most extended methodology.
2. Appropriate mode—iterative method.
3. Modal identification and combined imperfection—coupled FEM/GBT method.

Then they have been compared with experimental results.

The first two alternatives use only the finite element method. In the third alternative, two different techniques will be combined, the generalised beam theory to generate the geometry imperfection and the finite element method to carry out the nonlinear simulation.

Is important to know that the use of (1) and (3) are recommended for lengths where distortional buckling is predominant and a methodology that couples two techniques, FEM and GBT, has been developed. The FE method provides the buckling modes (linear eigenbuckling analysis) and the ultimate load (non-linear analysis). By GBT the modal identification is made, which allows generating a combined geometric imperfection in a more rational way. In this study is only tested one shape of cross-section.

In 2012, has made a study [9] that introduces which methods can be used to analyse the efforts pallet cold-formed steel storage structures with perforations. Consisting of cold-formed angle sections with perforations are difficult to analysed because of these perforations and because the computational results aren't certainly valid. For this reason, the design of these structures is based on experimental tests prescribed by specific codes. The European design code allows for the use of numerical approaches that takes rational account the influence of perforations (i.e. Finite Element Analysis), providing that the models are validated by relevant tests.

In this paper analytical and numerical based methods have been proposed although all have to be compared with experimental methods. Direct Strength Method (DSM) is a very good method but even that, if a good agreement between the DSM predictions and experimental testing exists, it is still not possible to avoid testing. In this report we can see the different ways to study these members (experimental or numeric methods): The European Standard EN1993-1-3:2006 (but doesn't consider the holes), European Standard EN15512:2009, Generalized Beam Theory (GBT), Finite Element Methods (FEM) and some more else.

In this study one shape of cross-section is tested but with different dimensions. Something noteworthy about the perforated specimens studied in this paper is the study of the residual stresses which were determinate using the method proposed by Rondal, which allows the determination of flexural residual stresses on both interior and exterior faces of cold-formed profiles by direct geometric measurements of the curvature of a strip cut off from a profile. Finally is demonstrated by comparison that the realization of many experimental tests to the design of these elements is not necessary [9].

In the same year one article of optimisation was published [10]. The study presents the optimisation of cold-formed steel open columns using the recently developed self-shape optimisation method that aims to discover new profile shapes. The shape of the cross-section is very important and despite the manufacturing process allowing achievement of almost any desired cross-sections, only conventional C, Z or S cross-sectional shapes are normally used in practice. With a new method the use of a variety of profiles is allowed and some sections with different forms allowing them to be the optimum. An automatic determination of the elastic buckling stresses of cold-formed steel profiles for optimisation purposes is challenging as “engineering judgement”, is often needed to select the appropriate buckling value when elastic buckling analyses fail to directly identify a mode. This paper presents a clear set of rules to obtain the local and distortional elastic buckling stresses using the Finite Strip Method (FSM) and constrained Finite Strip Method (cFSM). As a result we can know that the rounded shapes have the advantages of increasing the local buckling strength while maximising the global buckling strength. But on the limitations of drawing curves computationally the optimal shape of the cross-section cannot be made directly. Because of that the shape is manually drawn before computationally. This is the self-shape optimisation principle, that it will be extended in the future to incorporate the moment capacity  $M_c$  estimated from the DSM in the fitness function  $f$ , in a similar manner to the axial capacity  $N_c$ .

Finally the evaluation made in 2013 by Andrei Crisan, Viorel Ungureanu, Dan Dubina, [11] is about global buckling behaviour, with or without interaction with distortional buckling tests carried out according to the EN 15512 (2009) on compression. It is based on tests completed with numerical analysis. The present paper attempts to demonstrate that the design buckling strength of uprights can be conveniently estimated by single section tests, providing that the length of these members is calibrated for the distortional–global interaction mode. Even though in recent years numerous investigations have been devoted to the effects of holes and member slenderness on the ultimate capacity of pallet rack uprights, no analytical method for the design of rack structures is generally accepted. For this reason, the design of these structures is based on experimental tests

prescribed by specific codes. Is an experimental and analytical program for testing two different shapes of the section.





## **PART**

### **II. Methods and development**



### 3. Methodology

#### 3.1. Optimisation problem formulation

On the present work the optimisation problem consists in the increasing of the stiffness and in the reduction of cost of the structure.

In order to accomplish it a design of experiments (DOE) methodology and a Response Surface Method (RSM) will be used as tools to find the optimum value of stiffness and cost.

In order to get it, an objective function ( $F$ ) that varies according to a set of variables (variable factors:  $x_1, x_2, \dots, x_n$ ) that have been previously selected is chosen. This function will be maximized (or minimized) thus obtaining the values of the design variables in order to obtain the optimal structure.

The optimization process is going to be applied as follows:

- 1) Creating a design of experiments → Set of experiments planned in advance with given values of the variables.
- 2) Model adjustment → mathematical equation that connects the response between the factors studied.
- 3) Using an optimization method → The model is explored to get information about the optimal.

In the procedure, there are some design variables which are going to be modified ( $x_1, x_2, \dots, x_n$ ). In order to analysed how these variables affect the structure, a numerical simulation model (ABAQUS) will be used. Therefore, the design structure is created in the software (ABAQUS) and it is simulated as many times as the design variables are changed.

##### 3.1.1. Design of experiments (DOE)

In order to analysed a determined system, mathematical and statistical methods can be used. One of those methods is the Design of Experiments (DOE), which recently has been applied to decide how many experiments are necessary to do a good evaluation of the specimen. DOE determines the allocation and method of experiments to satisfy the objectives, doing an efficient analysis of the results. In other words, it studies how varied the usual conditions for an empirical process to increase the probability of detecting significant changes in the response; this way it is gotten a better understanding of the process behaviour of interest.

This method works with characteristic value that is equivalent to the objective function and factors those are equivalent to design variables of the design. This function is the response of these factors.

The function can be approximated by some specific function values. Suppose we have a function  $F$  with design variable vector  $b$ , as follows:

$$F = f(b) = (x_1, x_2, \dots, x_n) \quad (3.1.)$$

The vector  $b$  is constructed by the variables factors  $(x_1, x_2, \dots, x_n)$  which influence the function  $F$ . These variable factors are chosen in the design and they are modified during the experiments. They can be factors of geometry, temperature, time, etc., depend on the experiment. The values that the variables factors adopt are called “levels”, each variable factor will have the amount of levels that it is considered to obtain a good result.

Two methods are then usually used: (1) the orthogonal arrays method and (2) the response surface method (RSM), which uses the methamodel of explicit functions for approximation.

In general, the design of experiments for systems where there are one or more variables of response ( $F$ ) whose value depends on one or more controllable independent variables ( $x$ ), called factors applied. Responses may be influenced by other uncontrolled variables.

### 3.1.2. Response surface method (RSM)

The response surface methodology (RSM) is an approximation method. It is a set of mathematical techniques used in the treatment of problems in which a response of interest is influenced by several factors quantitative.

The initial purpose of these techniques is design an experiment to provide reasonable values of the response variable, and then it is determined the mathematical model that best fits the data.



Figure 3.1. – Representation of RSM methodology.

The function expressed in 3.1. is going to be approximated and then it is going to be represented as the real response surfaced.

The structure of  $F$  that determinates the relationship between the factors and the response variable, is unknown. Therefore the first aim of the RSM is to establish experimentally an appropriate approximation of the function  $F$ . In order to solve this problem it is proposed a model for the equation. It is usually a polynomial model.

The function  $F$  is approximated using the optimization process. First, the following aspects should be determined:

1. Selection of the candidate points to generate the response surface, those can be selected by a DOE methodology.
2. The method to generate the response surface with the candidate points.
3. The optimization method to use with the response surface.

The function can be approximated by a cubic, a higher polynomial or a special function.

In order to achieve the ultimate goal, and after the generation of the Response Surface, an optimization method can be used to find the minimums or maximums of the Response Surface. It is expected that these values would be near the required solutions of the real system (modelled as a response model).

The Response Surface Method (RSM) is a sequential technique. Often, the initial estimate optimal operation conditions is far from the real optimum, so the goal is moving quickly unto the optimum. It is done using the simplest and least expensive method possible.

In the figure 3.2 it is explained the general methodology. At first the experimental data are obtained applying the design of experiments (DOE). Then a set of mathematical and statistical techniques is used in order to made a model. Finally the behaviour of a response surface is analysed applying an optimization method.

In the results chapter this process is explained in more detail, applying it to our particular case. The response surface  $F$  and the design variables are selected for the specific case.

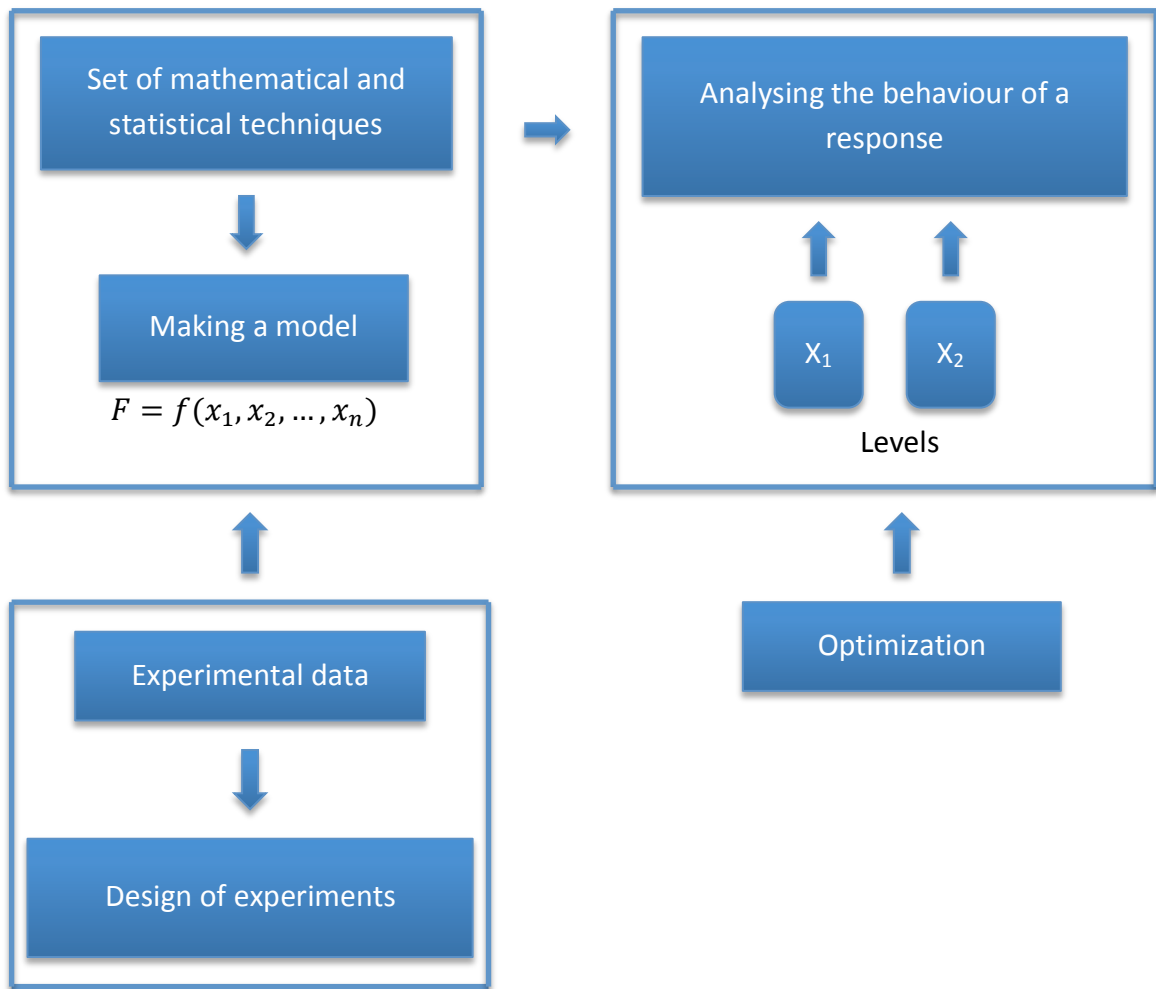


Figure 3.2. - Simple schema of the optimization method used in this work.

## **PART**

### **III. Results**





#### 4. Description of the problem

In the specific problem of this work, the increase of the stiffness of a thin sheet structure for storing is required, however an affordable and proportionate cost should be taken in account.

The structure that is wanted to be optimized it is made of steel S355 with the section and dimensions presented in figure 4.1. Some useful measurements of the initial structure are listed in the table 4.1.

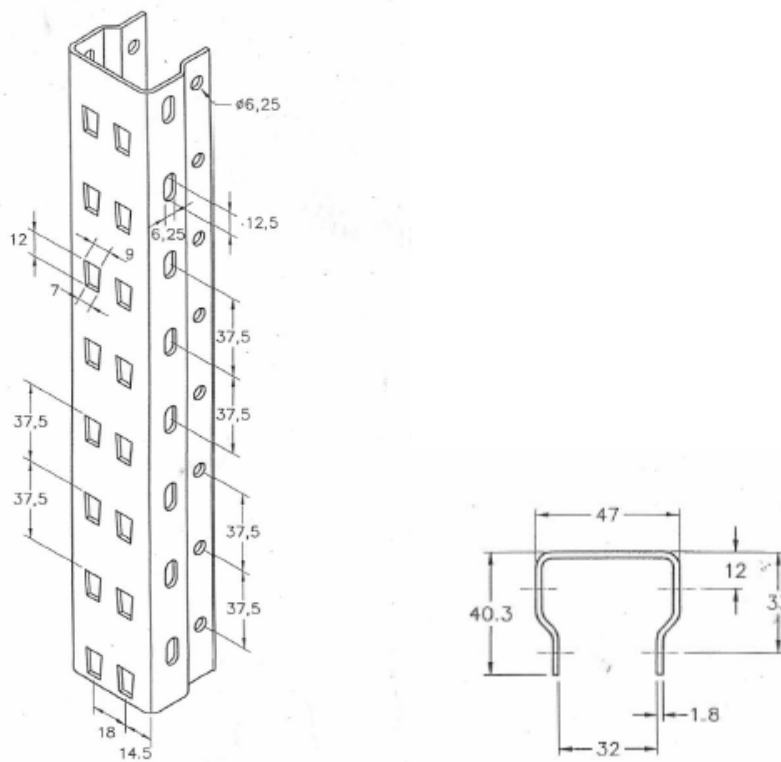


Figure 4.1. – Sections of the selected structure.

<b>Longitude (mm)</b>	375
<b>Thickness (mm)</b>	1.8
<b>Angle (°)</b>	106.89
<b>Number of holes</b>	10

Table 4.1. – Characteristic values of the structure.

The three types of holes are always presented in the same number (10) each one.

The properties of the material (steel EN S355) that are going to be used in this work are listed in the table 4.2.

<b>Poisson's Ratio</b>	0.30
<b>Elastic Modulus (GPa)</b>	190
<b>Tensile Strength (Mpa)</b>	1158
<b>Yield Strength (Mpa)</b>	1034
<b>Elongation (%)</b>	15
<b>Reduction in Area (%)</b>	53
<b>Hardness (HB)</b>	335
<b>Density (Kg/m3)</b>	7850

Table 4.2. – Values of the material's properties.

In this work, the simulation of an experimental trail, as shown in figure 4.2 is accomplished. In figure 4.2., on the right side, images of the trail in the laboratory is presented. On the left of the figure, the schema that was modelled on Abaqus is depicted.

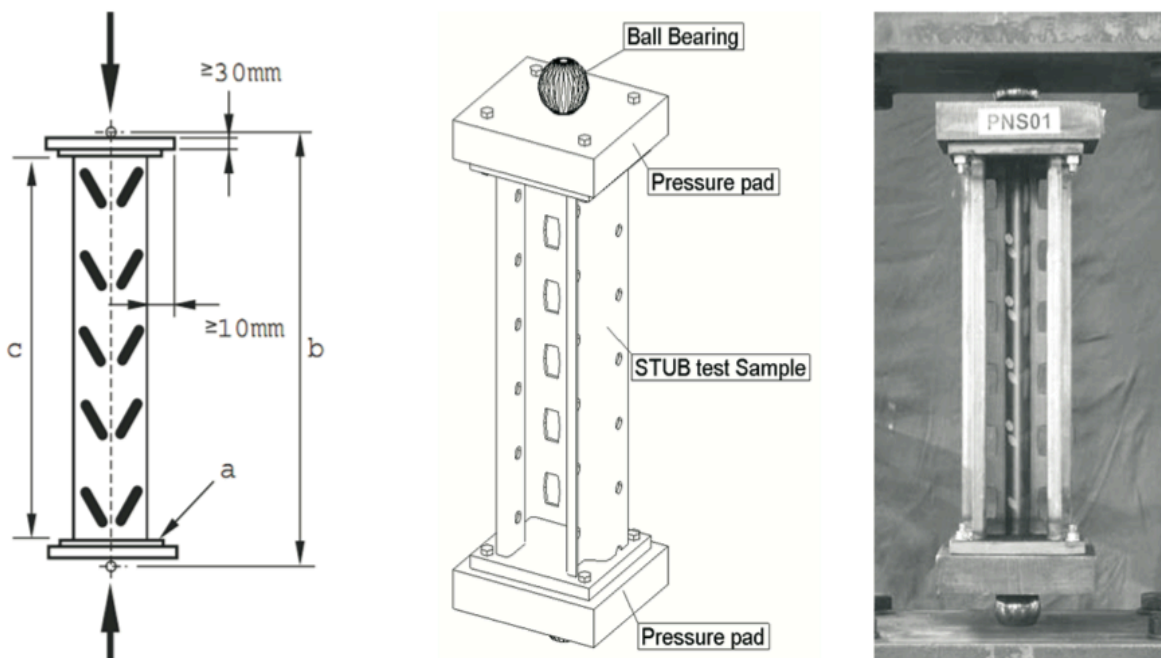


Figure 4.2. - Stub column test setup

## 5. Modelling

The structural problem is analysed through numerical simulation, using the FEM code Abaqus. Therefore, the necessary simulations are done and the results could be obtained and analysed.

The structure is created as approximate as possible to the real structure. As it is a symmetrical structure with respect to the longitudinal axis K, it is only simulated only half structure and symmetrical boundary condition is applied to facilitate the calculations.

First it is simulated the structure with the original dimensions (showed above), which is the model tested in the laboratory. Later the variables selected in the design of experiments (DOE) methodology are going to be changed one by one and several simulations are going to be made.

In ABAQUS, the structure, starting in the module part, is created. In this model, the section of the structure is designed parametrically and, later the parameters that are going to change will be modify in this module. The structure in the model part after being created is shown in the figure 5.1.

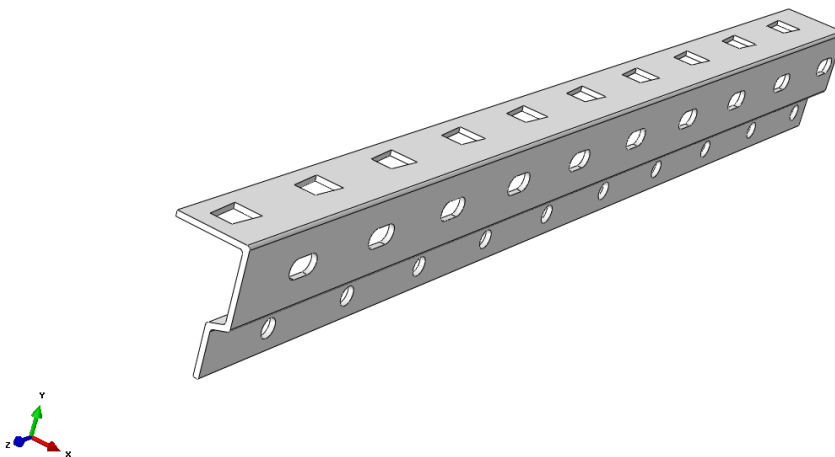


*Figure 5.1. – Design of the structure in the module part by ABAQUS.*

Once the structure is designed in ABAQUS and the material is assigned, the mesh is created. The material is assigned taking as initial hypothesis an elastic-perfect plastic behaviour to simplify as possible the numerical configuration and future results.

The mesh has to be created appropriately because the results largely depend on it. So, a mesh sensitivity study was done and the most efficient discretization can be seen in figure

5.2. The mesh is composed of tetrahedral 4 nodes-reduced integration elements. An homogeneous solid part was defined in Abaqus taking in account the properties of table 4.2.

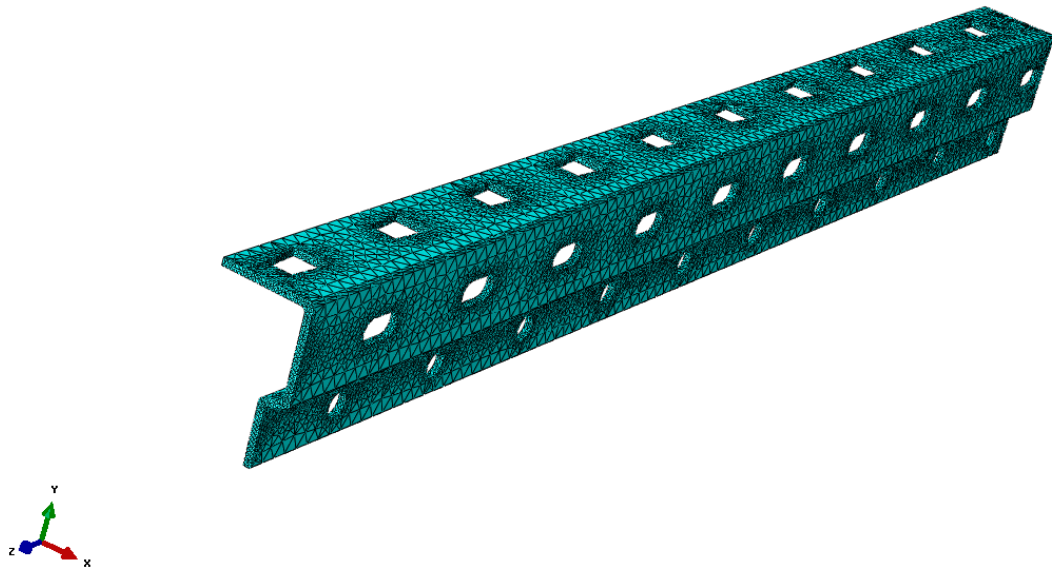


*Figure 5.2. – Design of the mesh of the structure by ABAQUS.*

The boundary conditions of the numerical model are the following:

1. Boundary condition of symmetry, in the  $k$  axis, modelling only half of the structure. It should be noticed that this condition is taken into account when manipulating data.
2. Boundary condition of encastre. One of the ends is fixed.
3. Boundary condition of displacement. Gradually apply a displacement for the deformation of the structure, as produced experimentally.

To apply the displacement, an analytical the end opposite of the encastre is used simulating the experimental test. These boundary conditions can be seen schematically represented in figure 5.3.

Then it is used a reference point in which a displacement of 4 mm in the direction of axis  $k$  is applied. The value of the displacement of 4 mm is chosen because the experimental results show that after this value the structure is plastically deformed. At the point of 4 mm of displacement the results are retrieved.

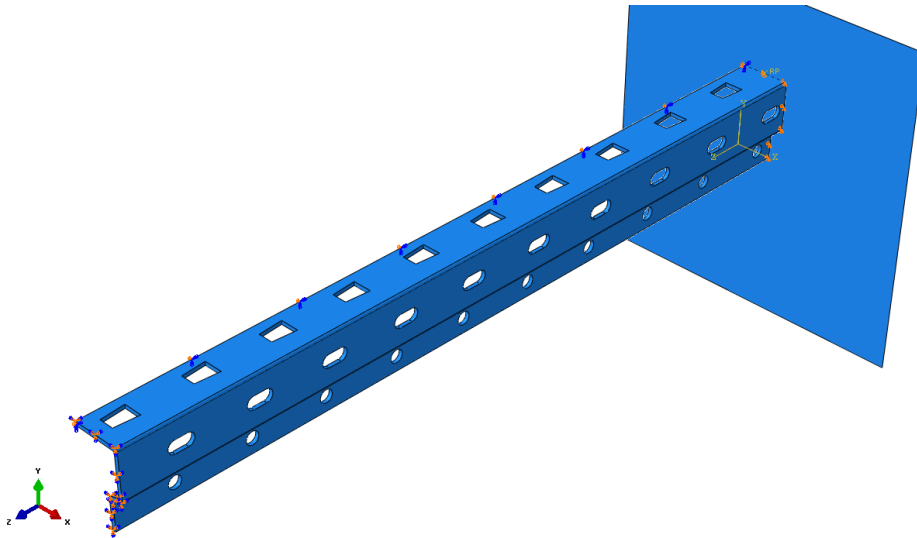


Figure 5.3. – Design of the assembly of the design.

## 6. Experimental results

In order to have a better knowledge about the experimental behaviour the structure was tested.

Figure 6.1 shows the structure located between two plates at the beginning of the test. Then, one of these plates moves until the plastic deformation of the structure is plastically deformed (figure 6.2).



Figure 6.1. – The structure in the laboratory without being submitted to any load.

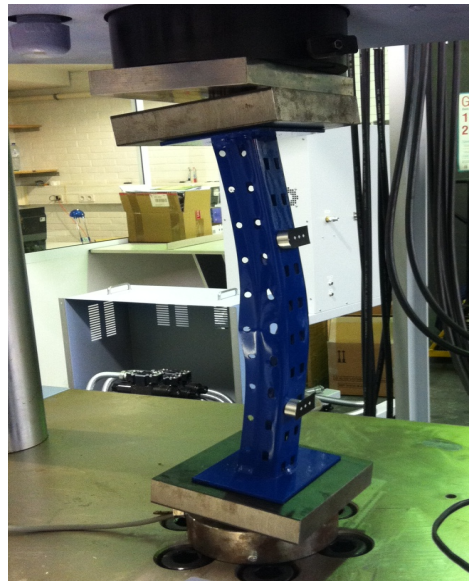


Figure 6.2. – The structure after being submitted to the load.

## 7. Model calibration

In order to validate the numerical model their results must be compared with experimental tests. Subsequently, the numerical, and its properties, can be calibrated with the porpoise of obtaining a good reproducibility.

The Young's modulus and the poisson coefficient, that are in the range of 190-210 MPa and [0.27-0.30] for tis material, can be determined in order to approximate the experimental curve obtained at the laboratory and curve obtained with the results taken from the simulation.

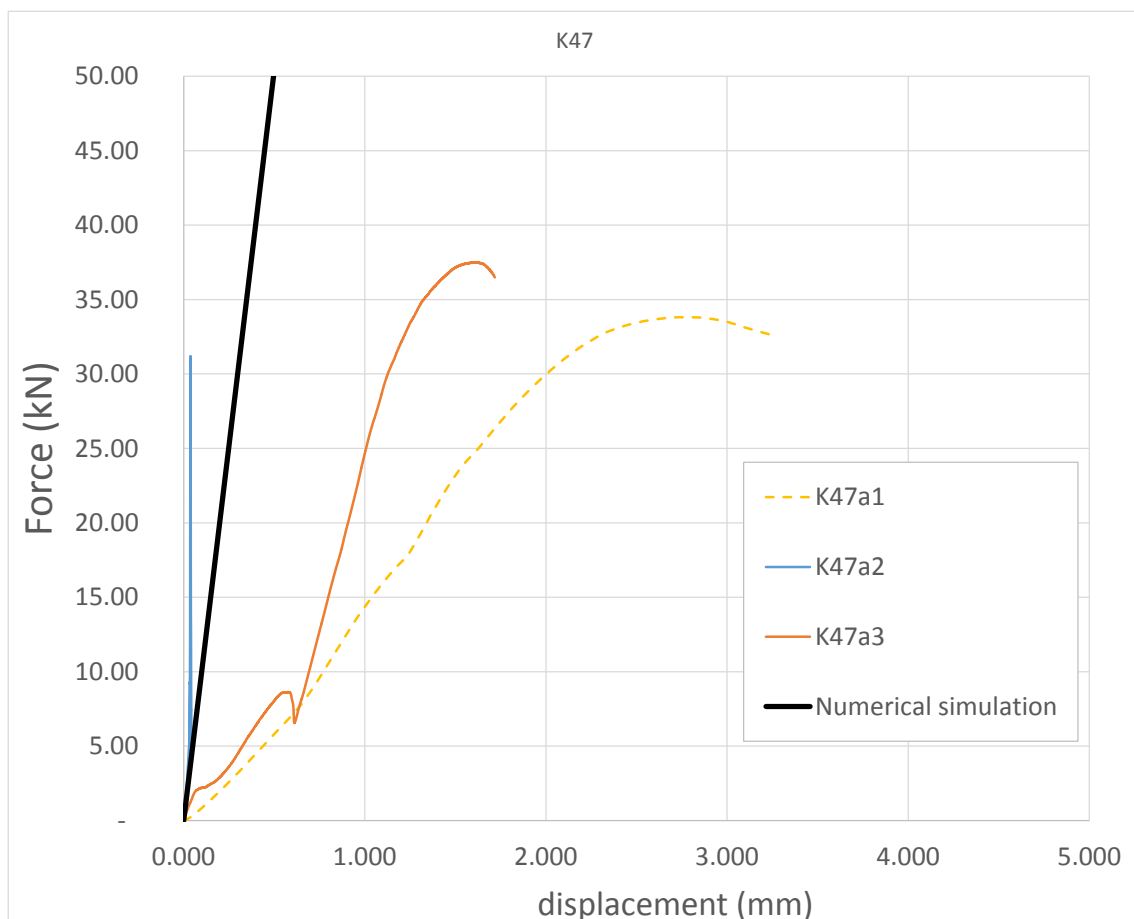


Figure 7.1. – The comparison between experimental and numerical curves.

The Young's modulus and poisson coefficient were adjusted to characterize the best the material and to reproduce the experimental tests. However, the large diversity of experimental results does not allow to make a precise calibration process.

## 8. Optimisation formulation

On the one hand it will be used ABAQUS software, where it will be simulated our problem. By the other hand, it will be applied a methodology to optimize the structure studied that includes, Design of Experiment (DOE) and the Response Surface Method (RSM).

As it is said before, the aim of this study is to find the optimum point of stiffness and cost. In order to do it, some variables which affect these parameters are going to be selected.

These design variables will be used in the process of Design of Experiments (DOE).

In this project the chosen design variables are: the angle of the inclination of the section ( $\alpha$ ), the thickness of the plate (t) and the number of holes (n).

It is known that the stiffness coefficient depends on the applied load and the displacement produced, which depend on the section of the structure. Furthermore, the cost depends on the amount of material (mass or volume), on the number of manufacturing operations and on the type of material.

As the piece must satisfy certain requirements concerning its shape, the number of manufactured operations is going to be considered the same for all the simulations. Therefore, no importance is given this parameter. However, it should be noticed that the cost increases with the number of manufacturing operations.

In order to observe how these three variables affect the behaviour of the structure, the Design of Experiments method (DOE) is used. This method indicates that some variables, some levels and a function have to be chosen. The levels are the values assigned to each one. In this case three levels for each one are assigned, one upper and one lowest. Following this method the number of simulations have to be  $3^n$ , in this case it will be  $3^3 = 27$ , as expressed the table 8.1.

The angle defined in table 8.1 is measured from the section as it is shown in figure 8.1.

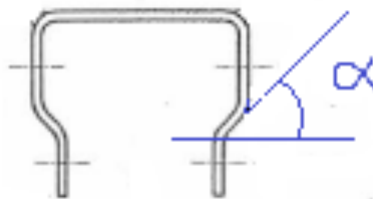


Figure 8.1. – Angle for the calculations ( $\alpha$ )

In the simulations it also has been added the value of the angle  $0^\circ$  in order to have a better description of the design variable  $\alpha$  in the proximity of 0. Then a total of 36 simulations were obtained.

The objective function, which depends on these variables, should be maximized. This function can be written as:

$$F_{obj} = (1 - \gamma)S + \gamma(-\$), \quad (8.1)$$

Where  $\$$  is the cost function and it is depend on  $n$ ,  $t$  and  $\alpha$ :  $\$ = f(n, t, \alpha)$ , and  $S$  is the stiffness function which is depend on the same variables:  $S = f(n, t, \alpha)$ .  $\gamma$  is a variable that takes the values of the weight it is wanted to have  $\$$  and  $S$ . At first the stiffness and the cost for each simulation is calculated and the Response Surface Method (RSM) is applied.

## 9. Experiments and results

In figure 9.1 it is observed the structure after applying a displacement of 4 mm. By the values of the stress, it cab be seen that the structure obtained is plastically deformed.

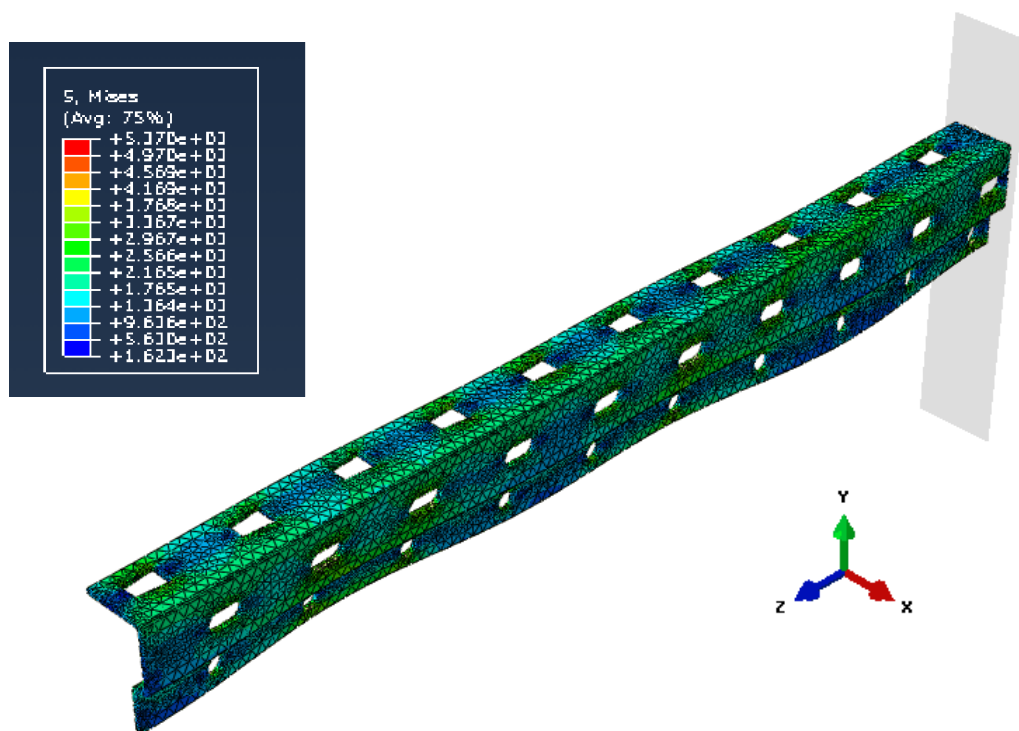


Figure 9.1. – The results in abaqus of the simulated structure.



Number of experiments\Variables	n	t	$\alpha$
32	5	1,2	0
13	5	1,2	16,89
14	5	1,2	22,5
15	5	1,2	45
31	5	1,8	0
10	5	1,8	16,89
11	5	1,8	22,5
12	5	1,8	45
33	5	2,4	0
16	5	2,4	16,89
17	5	2,4	22,5
18	5	2,4	45
29	10	1,2	0
4	10	1,2	16,89
5	10	1,2	22,5
6	10	1,2	45
28	10	1,8	0
1	10	1,8	16,89
2	10	1,8	22,5
3	10	1,8	45
30	10	2,4	0
7	10	2,4	16,89
8	10	2,4	22,5
9	10	2,4	45
35	15	1,2	0
22	15	1,2	16,89
23	15	1,2	22,5
24	15	1,2	45
34	15	1,8	0
19	15	1,8	16,89
20	15	1,8	22,5
21	15	1,8	45
36	15	2,4	0
25	15	2,4	16,89
26	15	2,4	22,5
27	15	2,4	45

Table 8.1. – Design of experiment for this experiment.

The other 35 types of structures and their curves of load-displacement are compared. A comparison in groups is made in order to clearly show the results.

The first division is based on the number of holes (5, 10, 15). The structures with 5 holes are compared in groups depending on the thickness. By these figures, it is shown that the stiffness of the structure varies according to the angle.

It can be observed that the better cases are the ones designed by an angle of 90°. About thickness, the stiffness increases with the increase of thickness. The simulations with 10 and 15 holes show the same, corroborating the same conclusions.

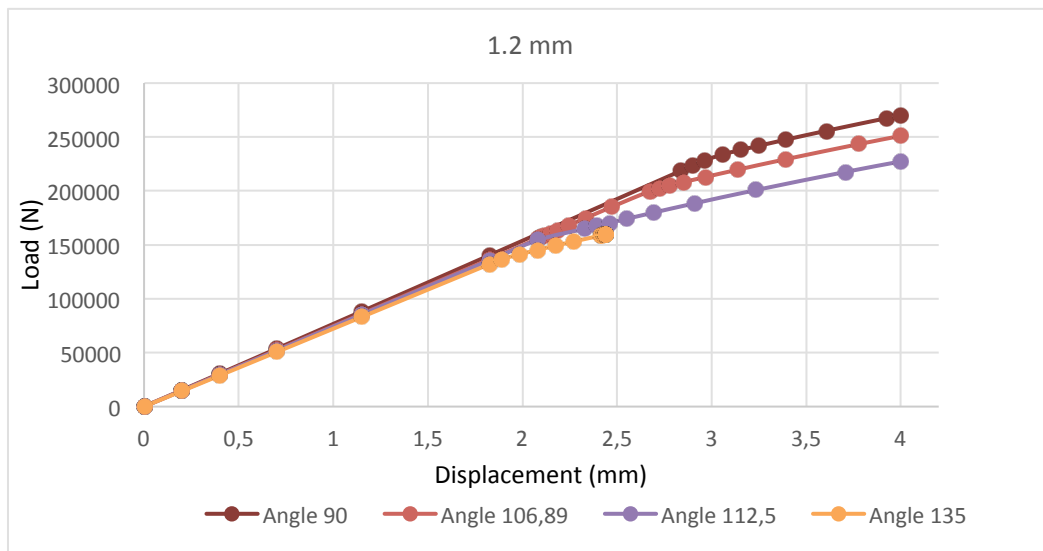


Figure 9.3. – Curve load-displacement for 5 holes and thickness of 1.2 mm.

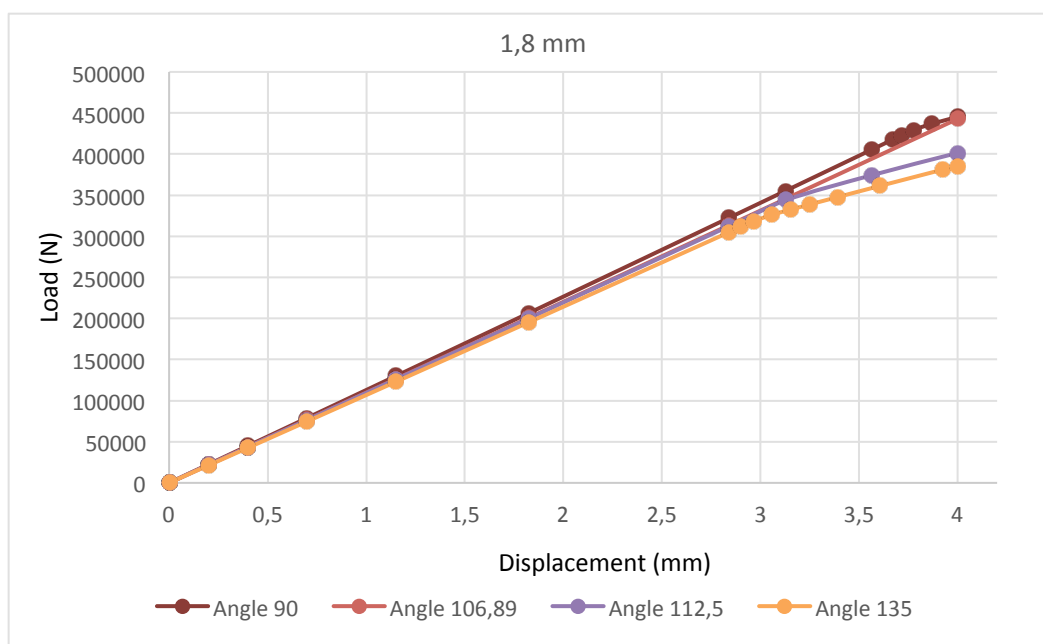


Figure 9.4. – Curve load-displacement for 5 holes and thickness of 1.8 mm.

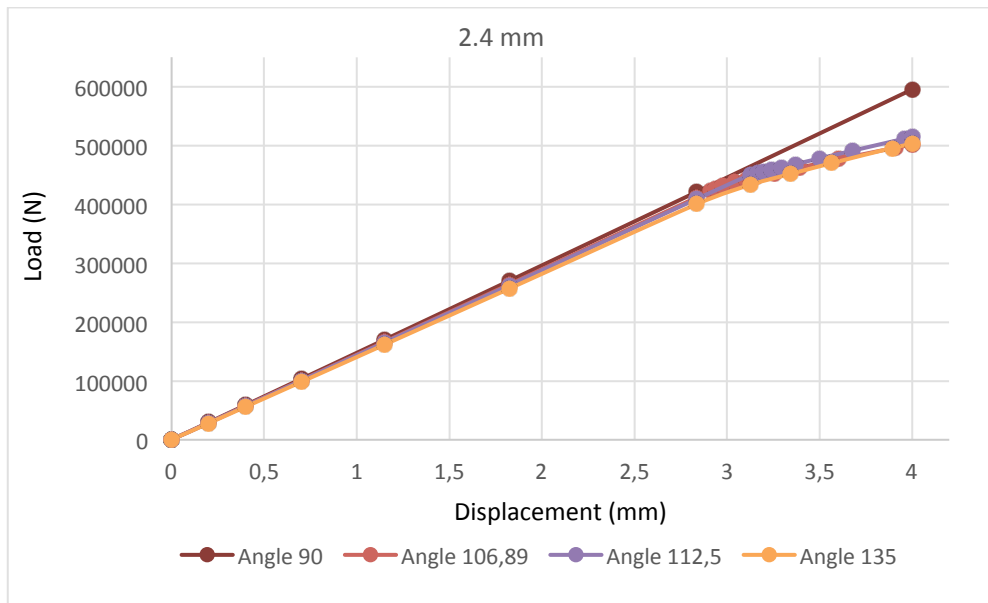


Figure 9.5. – Curve load-displacement for 5 holes and thickness of 2.4 mm.

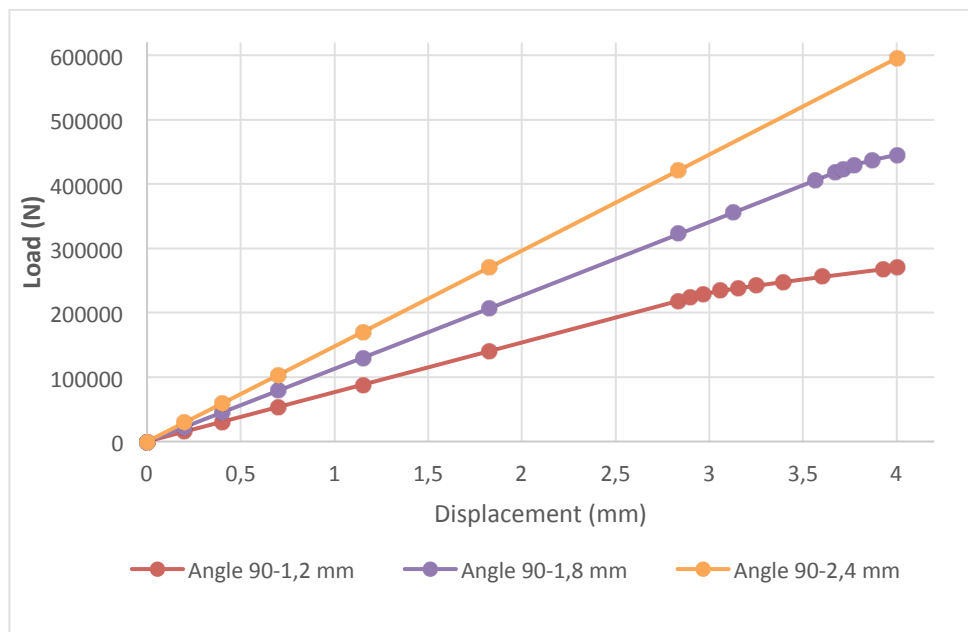


Figure 9.6. – Curve load-displacement for 5 holes and angle of 0.

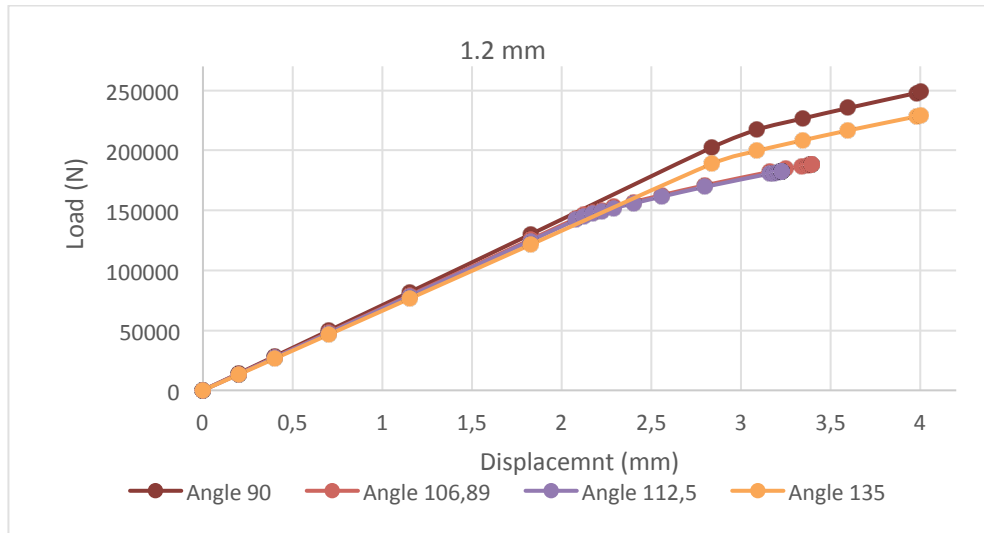


Figure 9.47. – Curve load-displacement for 10 holes and thickness of 1.2 mm.

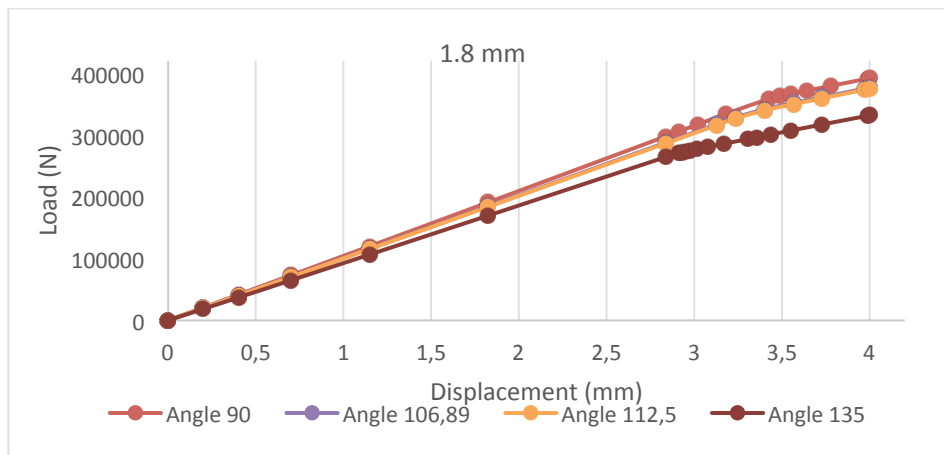


Figure 9.8. – Curve load-displacement for 10 holes and thickness of 1.8 mm.

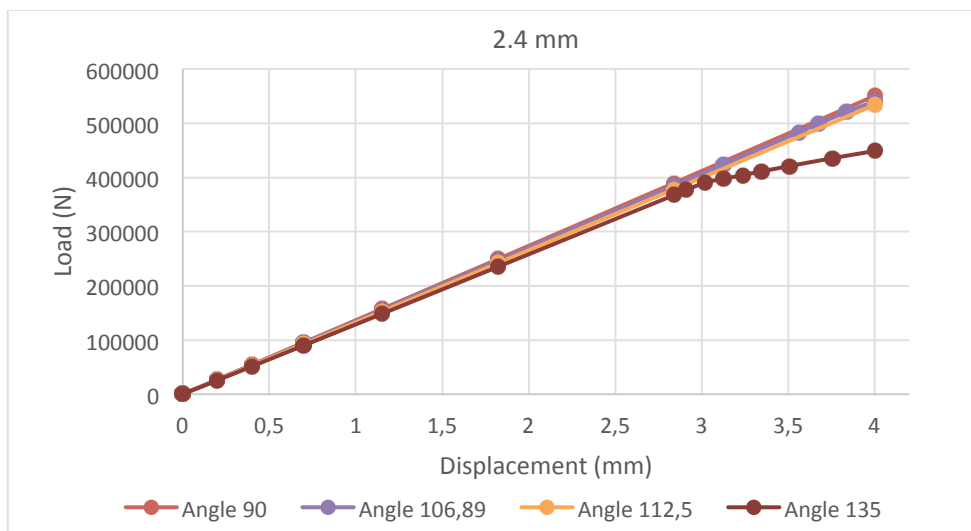


Figure 9.9. – Curve load-displacement for 10 holes and thickness of 2.4 mm.

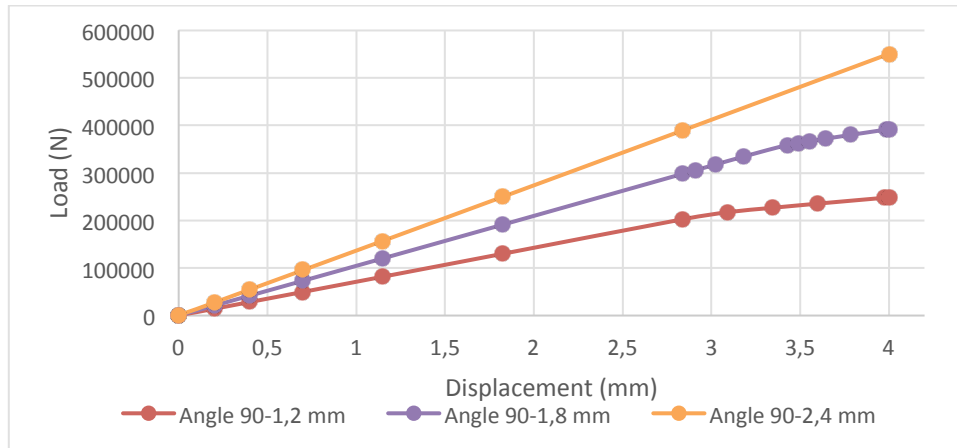


Figure 9.10. – Curve load-displacement for 10 holes and angle of 0.

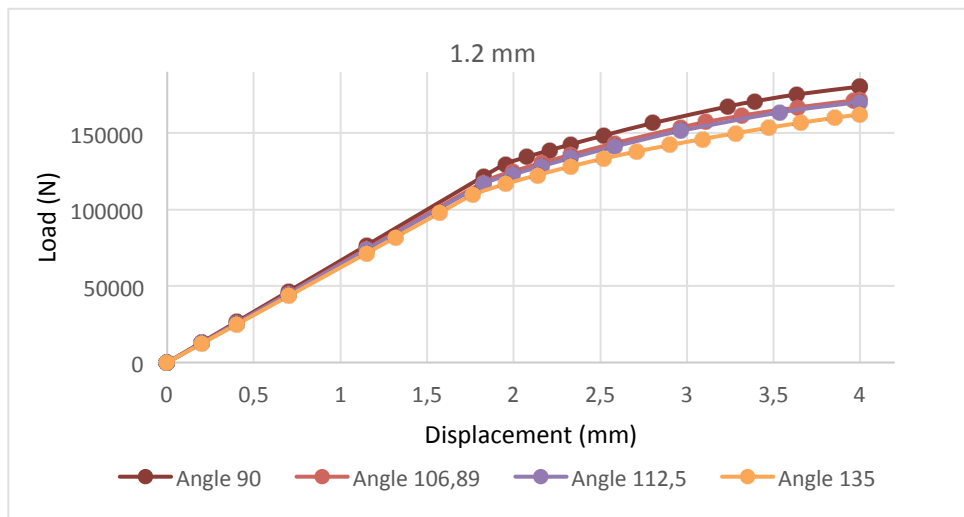


Figure 9.11. – Curve load-displacement for 15 holes and thickness of 1.2 mm

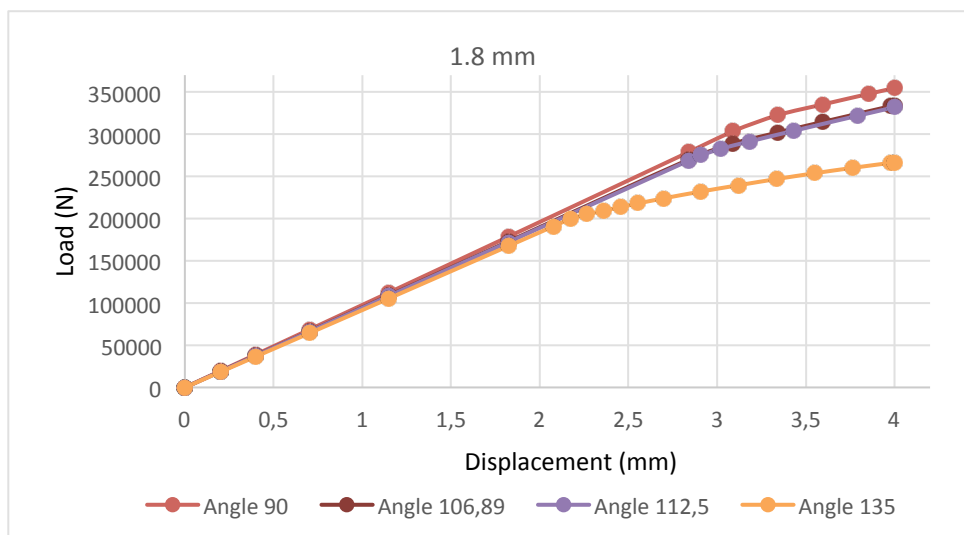


Figure 9.12. – Curve load-displacement for 15 holes and thickness of 1.8 mm

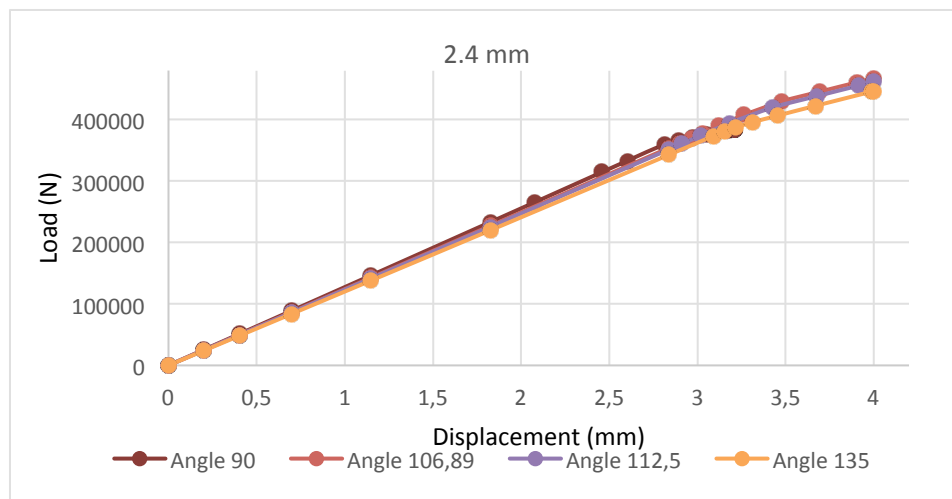


Figure 9.13. – Curve load-displacement for 15 holes and thickness of 2.4 mm

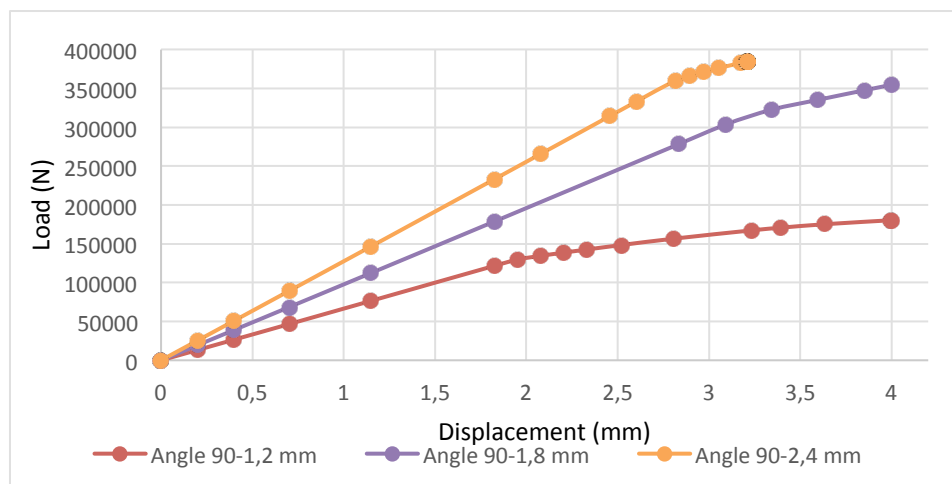


Figure 9.14. – Curve load-displacement for 15 holes and angle of 0.

## 10. RSM and final value

In this section, the Response Surface Method (RSM) is applied. As is said above, it has been already selected the variables and the objective function and then it is calculated the stiffness and the cost for each simulation. The results are shown in the table 10.1. This method is applied as schematically shown in the figure 10.1.

It is shown that the objective function depends on  $n$  (number of holes),  $t$  (thickness),  $\alpha$  (angle) and  $\gamma$  (weight). To calculate the stiffness the curves load-displacement of each simulation were used. It is known that the stiffness can be approximated to the slope of the curve by the following way:

$$S = \frac{L}{d} \quad (10.1.)$$

where  $L$  is the applied load and  $d$  is the displacement produced by the applied load.

Although in this case a displacement is applied and the load is consequently taken.

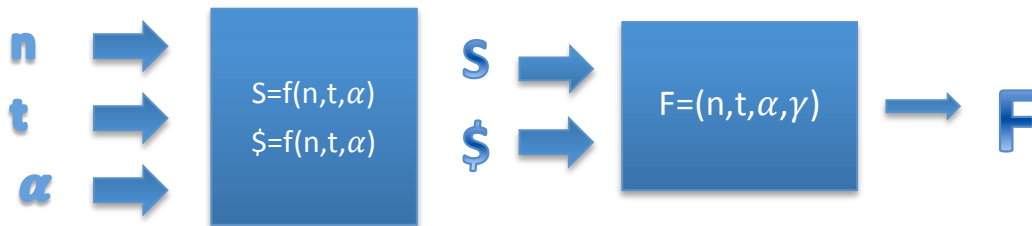


Figure 10.1. – Schema of RSM method to obtain a response model function  $F$ .

Equation 10.1 is used to calculate in each simulation, however, is obtained the average for all the values is taken. So one value of stiffness is obtained for each simulation.

To calculate the values of the cost in each simulation the volume of each structure is calculated and then multiplied by the specific cost of the material. The cost of the material is taken from the basis of construction prices from the Extremadura government [14] where the cost of steel S355 is 1,17 €/kg. By this way it is has an approximate price of each structure. As the structure has some manufacturing operation it is decided that the cost increases 10%, being this cost also proportional to the thickness. The results are shown in table 10.1.

The values of cost (\$) and stiffness ( $S$ ) are needed in the equation 10.1 to obtain the objective function. However, these values must be normalized in order to have the values of cost (\$) and the values of stiffness ( $S$ ) on the same order of magnitude.

For this purpose, the values of the stiffness are divided by a reference stiffness coefficient calculated using equation 10.2 and the values of the costs are divided by the lower of all the costs.

$$K = \frac{EA}{L} \quad (10.2.)$$

Where  $E$  is the Young module in the simulations,  $A$  is the approximate area of the transversal section and  $L$  is the longitude of the structure.

The resulted values are shown in table 10.2.

Number of experiments\ Variables	n	t (mm)	$\alpha$ (°)	Stiffness (N)	Cost (€)
32	5	1,2	0	74676,11679	0,297001375
13	5	1,2	16,89	72995,79234	0,289461442
14	5	1,2	22,5	68787,13962	0,287452587
15	5	1,2	45	68381,95564	0,280640428
31	5	1,8	0	113160,0358	0,437628151
10	5	1,8	16,89	110012,9743	0,42630878
11	5	1,8	22,5	108014,0681	0,424752541
12	5	1,8	45	104586,0366	0,415377224
33	5	2,4	0	147959,4939	0,572881366
16	5	2,4	16,89	140649,2535	0,560814284
17	5	2,4	22,5	140039,2744	0,557544288
18	5	2,4	45	136540,8891	0,546289719
29	10	1,2	0	68571,17495	0,286372891
4	10	1,2	16,89	62907,29103	0,2777732
5	10	1,2	22,5	62569,89027	0,275758364
6	10	1,2	45	63613,52674	0,268953183
28	10	1,8	0	103331,0021	0,421727795
1	10	1,8	16,89	99528,01528	0,411632679
2	10	1,8	22,5	99068,48373	0,407199243
3	10	1,8	45	91011,53235	0,397827913
30	10	2,4	0	136738,3928	0,5516892
7	10	2,4	16,89	135147,0774	0,545253888
8	10	2,4	22,5	132628,9022	0,536713017
9	10	2,4	45	125316,0948	0,52289529
35	15	1,2	0	58925,95043	0,273575043
22	15	1,2	16,89	56117,19724	0,266088946
23	15	1,2	22,5	57673,38431	0,264069125
24	15	1,2	45	53747,26882	0,257263944
34	15	1,8	0	95771,43941	0,402510587
19	15	1,8	16,89	91513,75328	0,391251034
20	15	1,8	22,5	91798,85048	0,389662892
21	15	1,8	45	83212,10741	0,380293556
36	15	2,4	0	123754,4705	0,526075561
25	15	2,4	16,89	123245,8544	0,514071286
26	15	2,4	22,5	121939,3746	0,5107654
27	15	2,4	45	118532,714	0,49951781

Table 10.1. – Values of stiffness and cost for each simulation.



Number of experiments\ Variables	n	t (mm)	$\alpha$ (°)	Normalized Stiffness	Normalized Cost
32	5	1,2	0	1,228225605	1,253133656
13	5	1,2	16,89	1,20058869	1,221320525
14	5	1,2	22,5	1,131367428	1,212844595
15	5	1,2	45	1,124703218	1,184102149
31	5	1,8	0	1,8611848	1,846478204
10	5	1,8	16,89	1,809423919	1,798718547
11	5	1,8	22,5	1,776547172	1,79215233
12	5	1,8	45	1,720165075	1,752595185
33	5	2,4	0	2,433544307	2,417150164
16	5	2,4	16,89	2,31331009	2,366235694
17	5	2,4	22,5	2,303277539	2,352438647
18	5	2,4	45	2,245738307	2,304952407
29	10	1,2	0	1,127815378	1,208289046
4	10	1,2	16,89	1,034659392	1,172004494
5	10	1,2	22,5	1,029110037	1,163503325
6	10	1,2	45	1,046275111	1,134790324
28	10	1,8	0	1,69952306	1,779390061
1	10	1,8	16,89	1,636973936	1,736795883
2	10	1,8	22,5	1,629415851	1,718089948
3	10	1,8	45	1,496900203	1,678549629
30	10	2,4	0	2,248986724	2,327734361
7	10	2,4	16,89	2,222813773	2,30058194
8	10	2,4	22,5	2,181396417	2,264545566
9	10	2,4	45	2,061119981	2,206244628
35	15	1,2	0	0,969176816	1,154291272
22	15	1,2	16,89	0,922980218	1,122705288
23	15	1,2	22,5	0,9485754	1,114183087
24	15	1,2	45	0,884001132	1,085470085
34	15	1,8	0	1,575188148	1,698307169
19	15	1,8	16,89	1,505160416	1,650799897
20	15	1,8	22,5	1,509849514	1,644099074
21	15	1,8	45	1,368620188	1,604567168
36	15	2,4	0	2,03543537	2,219663098
25	15	2,4	16,89	2,027069973	2,169013632
26	15	2,4	22,5	2,00558182	2,155065154
27	15	2,4	45	1,949551217	2,107608358

Table 10.2. – Values of the normalized cost and stiffness for each simulation.

The stiffness cost dependency of the design variables ( $n, t, \alpha$ ) must be analysed. The values of stiffness and cost versus thickness, number of holes and angle are represented in figures 10.2 to 10.7. The variation of stiffness cost with each variable factor can be analysed using these figures.

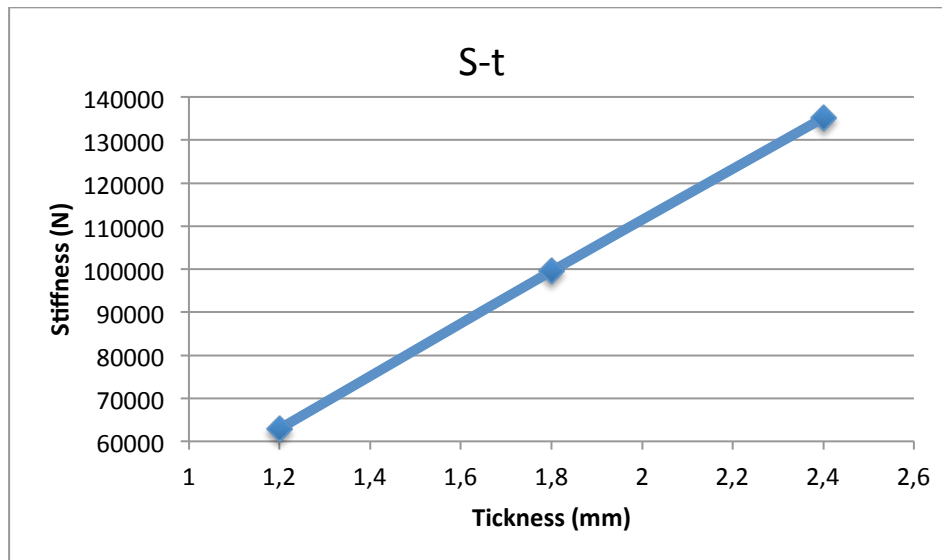


Figure 10.2. – Stiffness versus thickness. Number of holes = 10. Angles  $16.89^\circ$ .

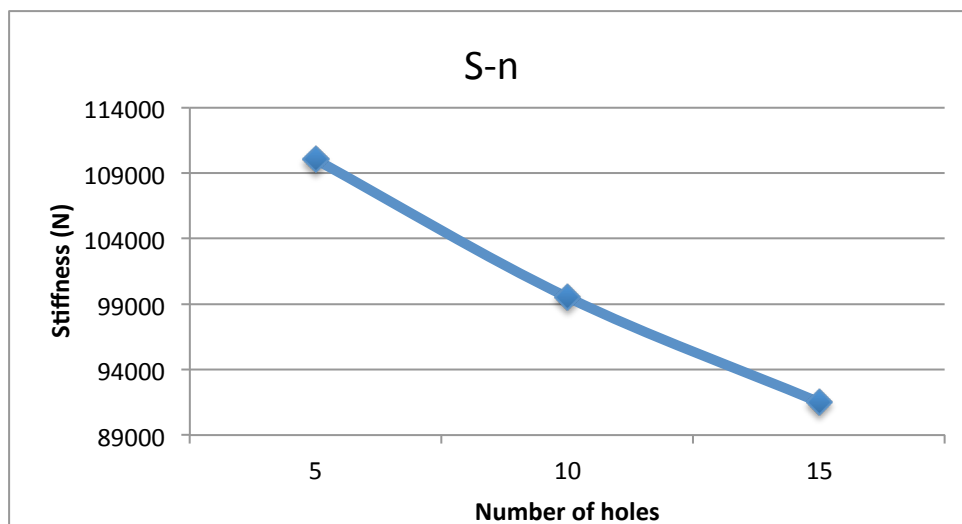


Figure 10.3. – Stiffness versus number of holes. Thickness = 1.8 mm. Angle =  $16.89^\circ$ .

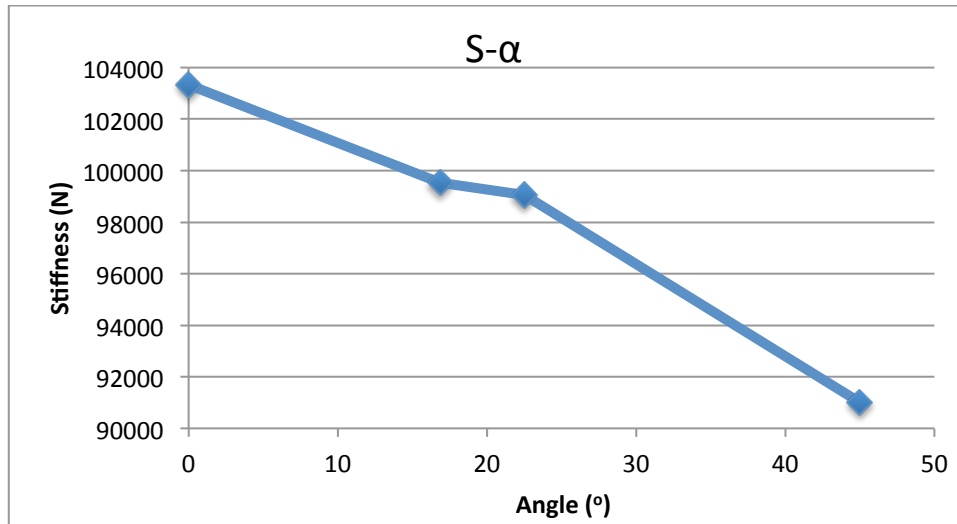


Figure 10.4. – Stiffness versus angle. Thickness = 1.8 mm. Number of holes = 10.

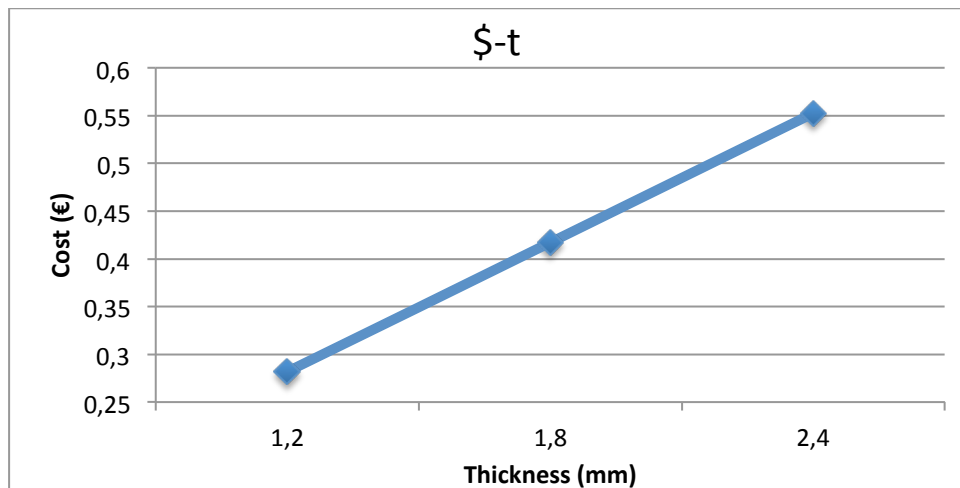


Figure 10.5. – Cost versus thickness. Number of holes = 10. Angles = 16.89(°).

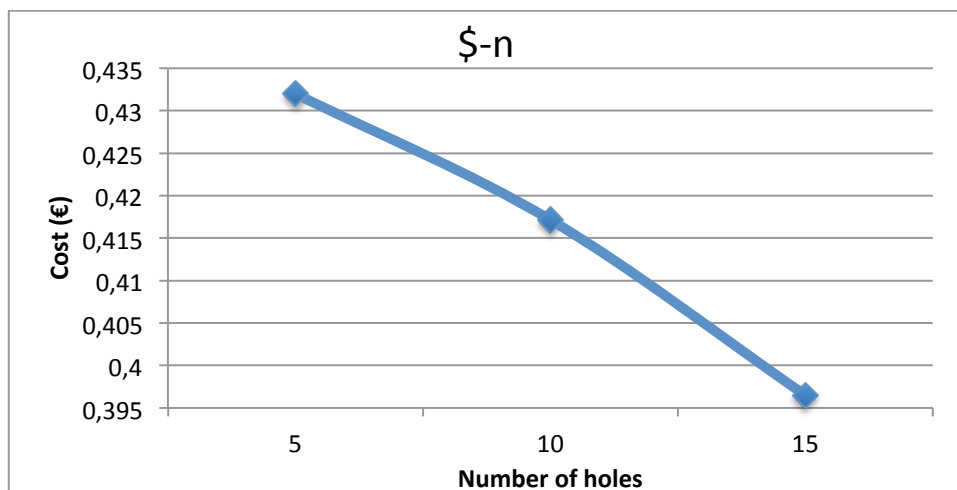


Figure 10.6. – Cost versus number of holes. Thickness = 1.8 mm. Angle = 16.89(°).

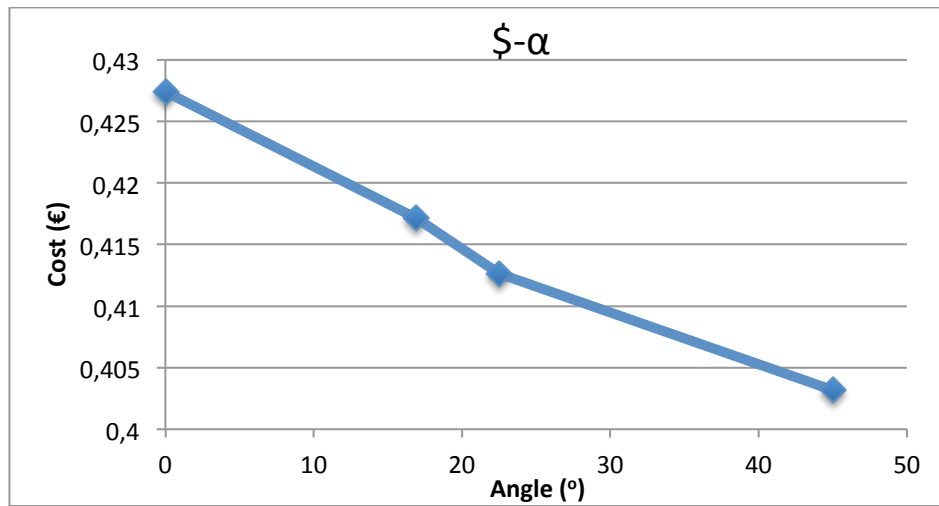


Figure 10.7. – Cost versus angle. Thickness = 1.8 mm. Number of holes = 10.

In order to find the response model of stiffness and cost according to their dependence on the design variables some coefficients must be calculated and fitted to the experiments results. The Response Surface Method here defined state that the Stiffness and the Cost depend on the design variables following this form of equations:

$$S = \beta_0 + \beta_1 n + \beta_2 t + \beta_3 \alpha + \beta_{12}(nt) + \beta_{13}(n\alpha) + \beta_{23}(t\alpha) + \beta_{11}n^2 + \beta_{22}t^2 + \beta_{33}\alpha^2 \quad (10.3.)$$

$$\$ = \varphi_0 + \varphi_1 n + \varphi_2 t + \varphi_3 \alpha + \varphi_{12}(nt) + \varphi_{13}(n\alpha) + \varphi_{23}(t\alpha) + \varphi_{11}n^2 + \varphi_{22}t^2 + \varphi_{33}\alpha^2 \quad (10.4.)$$

Using the excel software and the solver module the coefficients  $\beta$  and  $\varphi$  are going to be fitted as a least-square minimization problem. The resultant mathematical models, valid in the defined intervals of variation of controllable design variables are given by:

$$S = 0,158403049 - 0,018608196 \cdot n + 0,695567984 \cdot t - 0,001681822 \cdot \alpha - 0,00626668 \cdot (nt) + 0,0000533136 \cdot (n\alpha) - 0,001145672 \cdot (t\alpha) + 0,000575723 \cdot n^2 + 0,128137492 \cdot t^2 + 0,0000397976 \cdot \alpha^2 \quad (10.5.)$$

$$\$ = 0,115690294 - 0,000336397 \cdot n + 0,997150359 \cdot t - 0,001535532 \cdot \alpha - 0,006953191 \cdot (nt) - 6,60005E - 06 \cdot (n\alpha) - 0,00070511 \cdot (t\alpha) - 9,96676E - 05 \cdot n^2 - 0,000199335 \cdot t^2 + 1,61995E - 05 \cdot \alpha^2 \quad (10.6.)$$

With these equations the value of the objective function using a general  $n$ ,  $t$  and  $\alpha$  can be introduced in the equation 10.5 replacing  $S$  and  $\$$ .

$$F_{obj} = (1 - \gamma)S + \gamma(-\$) \quad (10.5.)$$

Some different results of the objective function can be obtained, depend on how many values  $\gamma$  takes. The final efficient solution is the one that maximize  $F_{obj}$ , maximizing the stiffness and minimizing the cost. Table 10.3 presents the optimized values found for several values of  $\gamma$ .

$\gamma$	$F_{obj}$
<b>0</b>	13,1274024
<b>0,1</b>	11,08108347
<b>0,2</b>	9,03476454
<b>0,3</b>	6,988445608
<b>0,4</b>	4,942126677
<b>0,5</b>	3,013519034
<b>0,6</b>	1,230062548
<b>0,7</b>	-0,071392802
<b>0,8</b>	-0,172251311
<b>0,9</b>	-0,272778351
<b>1</b>	-0,363000758

*Table 10.3. - Objective function values for different values of the weight  $\gamma$*

It is shown in the table 10.3 that the objective function has a larger value when the stiffness has more importance. This makes sense because the function it is defined with a positive member of the stiffness. So the value of the function decreases according to the weight given to the cost.

Then, this function was going to be optimized maximizing it and finding the best values for the variable factors: thickness, number of holes and the angle.

$\gamma$	0	0,1	0,2	0,3	0,4
<b>N.of holes (n)</b>	5	5	5	5	5
<b>Thickness (t)</b>	8	8	8	8	8
<b>Angle (<math>\alpha</math>)</b>	0	0	0	0	0
0,5	0,6	0,7	0,8	0,9	1
27,99994437 $\approx$ 28	28	28	28	28	28
8	8	0.5	0.5	0.5	0.5
89,99948089	90	90	90	84.40791895	63.90523884

Table 10.4. – Optimized values for each objective function obtained.

In table 10.4 it is shown that when the stiffness is more important than the cost, the thickness increases and the number of holes decreases. On the other hand, when the cost is more important than the stiffness, lower values of thickness are obtained while the number of hole is larger. When the stiffness and the cost have the same importance, it is verified the maximization of the number of holes, thickness and the angle.

In the figure 10.8 the cost and the stiffness are compared after being optimized. It can be seen that the inflection point is when the objection function gives the same importance for the cost as the stiffness.

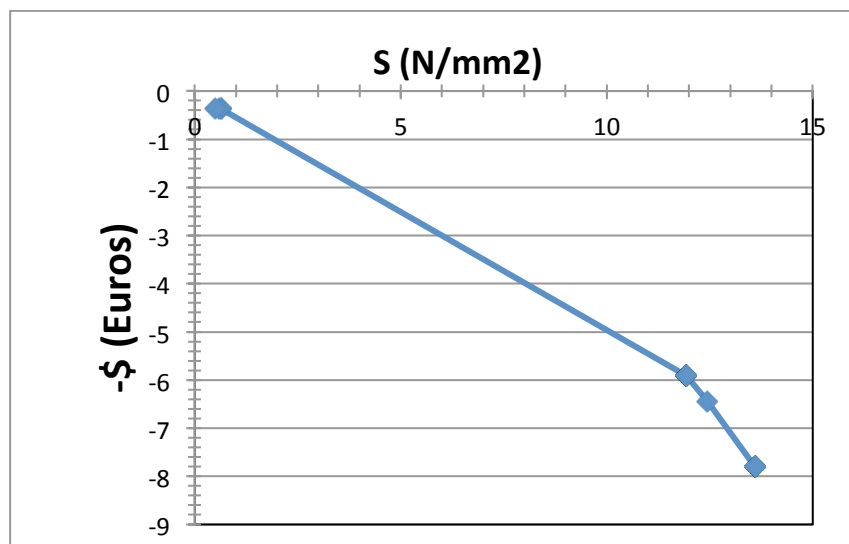


Figure 10.8. – Optimized cost versus stiffness (Pareto curve).

## **PART**

### **IV. Conclusion**





## 11. Conclusions

This work focuses on optimizing steel beam for storage with symmetrical sections and longitudinal pattern perforations.

The aim is to improve the stiffness of the structure under compression, important characteristic of the structure to comply its function. However it is important to pay attention to the price of the structure, important factor to optimize.

In order to implement this work some tools are used: a software for numerical simulation using finite element (ABAQUS) and optimization tools: design of experiments (DOE) and Surface Response Method (SRM).

Using the first tool the structure is created and submitted to compression, reproducing the experimental structure that has previously been performed in the laboratory. All the simulations needed for the work are carried out and the results are collected. Many of them represented as a load-displacement curve. The results allow to analyse the stiffness and compare with the experimental data. Some discrepancies were verified between the experimental and numerical results due to the lack of reproducibility of the experimental curves. Therefore, the numerical results were considered as reliable data taking into account that these reproduce the expected experimental behaviour.

The first optimization tool (DOE) is going to be used to decide which parameters of the structure are the key to study properly its behaviour. It is concluded that the most important parameters are the thickness, the number of holes and the angle from the cross section. As mentioned in the beginning of this study, the main purpose is not only studying the stiffness, but also the cost. Thus a new stiffness dependant cost function was defined by eq. 10.1.

The Response Surface Method (RSM) is used to find, on one hand, how the cost and stiffness depend on the variable factors and, on the other hand, the best values for these variable factors to optimize the structure.

These dependences were analysed using RSM method. By this analysis, it is observed that the stiffness depends on the design variables as a polynomial which is defined by unknowing coefficients. These coefficients are obtained using the Solver tool available on the excel software. The same procedure is applied for the cost function.

These functions are introduced into equation 10.1 to find the value of the objective function.

Finally the Solver tool is used again to optimize the value of the objective function. This function is maximized and is able to achieve the best values for thickness, number of holes and the slope angle.

The main results show that attributing the same importance to the stiffness and the cost, the design variables are larger and, consequently, it corresponds to the maximization of the number of holes, thickness and the angle.

# Bibliography

- [1] J. Rondal, “Cold formed steel members and structures General Report”, *Journal of Constructional Steel Research* 55 (2000) 155–158.
- [2] G.J. Hancock, “Cold-formed steel structures”, *Journal of Constructional Steel Research* 59 (2003) 473–487.
- [3] Murat Pala, Naci Caglar, “A parametric study for distortional buckling stress on cold-formed steel using a neural network”, *Journal of Constructional Steel Research* 63 (2007) 686–691.
- [4] M.M. Pastor, M. Casafont, E. Chillarón, A. Lusa, F. Roure, M.R. Somalo, “Optimization of cold-formed steel pallet racking cross-sections for flexural–torsional buckling with constraints on the geometry”, *Engineering Structures* 31 (2009) 2711–2722.
- [5] F. Roure, M.M. Pastor, M. Casafont, M.R. Somalo, “Stub column tests for racking design: Experimental testing, FE analysis and EC3”, *Thin-Walled Structures* 49 (2011) 167–184.
- [6] Benoit P. Gilbert, Kim J.R. Rasmussen, “Determination of the base plate stiffness and strength of steel storage racks”, *Journal of Constructional Steel Research* 67 (2011) 1031–1041.
- [7] Miquel Casafont, Maria Magdalena Pastor, Francesc Roure, Teoman Peköz, “An experimental investigation of distortional buckling of steel storage rack columns”, *Thin-Walled Structures* 49 (2011) 933–946.
- [8] J. Bonada, M. Casafont, F. Roure, M.M. Pastor, “Selection of the initial geometrical imperfection in nonlinear FE analysis of cold-formed steel rack columns”, *Thin-Walled Structures* 51 (2012) 99–111.
- [9] Andrei Crisan, Viorel Ungureanu, Dan Dubina, “Behaviour of cold-formed steel perforated sections in compression. Part 1—Experimental investigations”, *Thin-Walled Structures* 61 (2012) 86–96.

[10] Benoit P. Gilbert, Timothee J.-M. Savoyat, Lip H. Teh, *“Self-shape optimisation application: Optimisation of cold-formed steel columns”*, Thin-Walled Structures 60 (2012) 173–184.

[11] Andrei Crisan, Viorel Ungureanu, Dan Dubina, *“Behaviour of cold-formed steel perforated sections in compression. Part 1—Experimental investigations”*, Thin-Walled Structures 61 (2012) 86–96

[12] María Silva Cámara, María Mercedes de Zan, Luciana Vera Candiotti, Hector Goicochea, *“Temas de quiometría”*, Mayo 2013.

[13] Euebio Martínez, Manuel Estrems, Valentín Miguel, Antonio Garrido, José Antonio Guillén, *“Aplicación de la metodología de superficie de respuesta para la optimización de parámetros de soldadura en función de la distribución térmica resultante”*, XIII Congreso Internacional de Ingeniería de Proyectos Badajoz, 8-10 de julio de 2009.

[14] Base de precios de la construcción del gobierno de Extremadura.  
<http://basepreciosconstruccion.gobex.es/p/p03al/p03al.html>

[15] Viorel Ungureanu, Dan Dubina, *“Sensitivity to Imperfections of Perforated Pallet Rack Sections”*, Department of Steel Structures and Structural Mechanics Civil Engineering Faculty, University of Timisoara Ioan Curea 1, 300224 Timisoara, Romania. Laboratory of Steel Structures Romanian Academy – Timisoara Branch Mihai Viteazu 24, 300223 Timisoara, Romania. Mechanics and Mechanical Engineering. Vol. 17, No. 2 (2013) 207–220

[16] Gudelia Figueroa Preciado, *“Optimización de una superficie de respuesta utilizando jmp in”*, Departamento de Matemáticas Universidad de Sonora, Mosaicos Matemáticos No. 11, Diciembre, 2003.

[17] P. Teixeira a, A. Andrade-Campos, A.D. Santos, F.M.A. Pires, J.M.A. César de Sá. *“Optimization strategies for springback compensation in sheet metal forming”*. 24–27 April 2012, Aveiro. Portugal.

[18] Carmen Dolores Fernández Melcón, Montserrat Piñeiro Barcia. *“Superficies de respuesta. Métodos y diseños.”*